a. Specific Aims

Advancements in both neuroscience and engineering have provided neurosurgery with new paradigms for the restoration of neural function. In particular, the dual emergence of accurate stereotaxis and deep brain stimulation (DBS) have generated a revolution in the application of targeted neuromodulation. DBS allows for focused reversible inhibition of neural function, while advanced generation computers have made precise targeting and safe implantation through stereotaxis possible. Targeted neuromodulation is currently applied to a variety of movement disorders (1), but has shown the potential to provide novel treatments for epilepsy, eating disorders, obsessive compulsive disease, and pain (Appendix C). Nonetheless, because DBS depends on the focused delivery of electric current, it is incapable of pharmacological specificity and requires electronic neural prostheses that carry a significant complication rate.

Viral gene therapy has several advantages over DBS for the treatment of central nervous system (CNS) diseases. Rather than delivering electric current, viral vectors can alter synaptic function with molecular specificity. For example, delivery of the preproenkephalin gene to sensory neurons inhibits pain (2). Further, the genes for dopamine producing enzymes can correct models of Parkinson's disease (3). Viral vectors can also be constructed to deliver transgenes capable of promoting neuronal survival. For example, viral-mediated induction of glial derived neurotrophic factor and nerve growth factor are protective in models of Parkinson's (4) and Alzheimer's disease, respectively (5).

In addition to molecular specificity, vectors may be delivery to specific neuronal populations. Our recent data suggest that peripheral nervous system (PNS) injection of the adenoviral and adeno-associated viral vectors (rAAV) results in segmental delivery of recombinant genes to spinal cord sensory and motor neurons (6-8). Further, vector tropism can be modified to alter cell type tropism, creating the potential for system specific neuronal gene delivery (9). The experiments outlined in this proposal attempt to develop a vector capable of both neural tropism and neuromodulation. To test these concepts, we propose to develop a recombinant adeno-associated virus (rAAV) capable of synaptic inhibition and motor neuron tropism.

We have chosen the spinal reflex arc as a simple mammalian functional system amenable to neuromodulation. In addition, the functional disorder, *spasticity*, provides a target for the study of applied neuromodulation. The simplicity of the spinal reflex arc provides the potential for a better understanding of the mechanisms underlying gene-based neuromodulation. We hypothesize that an rAAV vector capable of specific motor neuron inhibition will have therapeutic efficacy in animal models of spasticity. In addition to providing a novel approach to spasticity, data from these studies will permit the rational design of rAAV vector(s) for application to motor neuron disease (ALS) and stereotactic neuromodulation. There are three aims:

1. **CONSTRUCT NOVEL VECTORS CAPABLE OF FOCUSED SYNAPTIC INHIBITION.**
   The light chain of TeTx has been shown to selectively block neural transmission via intracellular protease activity. Truncation of the wildtype toxin prevents this transgene from producing an active neurotoxin.
   a. Produce first generation adenovirus (Ad.RSVTeTxLC) containing an expression cassette of the 1.9 Kb TeTx LC under the control of the rous sarcoma virus (RSV) promoter by Cre-Lox *in vitro* recombination.
   b. Assay for TeTx activity in neuronal (SH-SY5Y cells) and nonneuronal cell lines (3T3 cells) infected with Ad.RSVTeTxLC using a rapid fluorescence based assay.
   c. Evaluate hindlimb motor function of rats following lumbar spinal cord and sciatic nerve Ad.RSVTeTxLC injection for proof of principle and evaluate the potential for pulmonary or hepatic toxicity.
   d. Construct an rAAV vector for the delivery of TeTxLC (rAAVRSVTeTxLC).
2. **DEVELOP STRATEGIES FOR TARGETED MOTOR NEURON DELIVERY OF rAAV ANTISPASTICITY TRANSGENES.**
   Enhanced neural uptake of rAAV-2 can be achieved through manipulation of the cap gene protein VP1.
   a. Construct mutants of the rAAV cap gene in pIM29-45 by inserting candidate peptides at aa34 of the VP1 protein.
   b. Evaluate the capacity of these strategies to enhance rAAV gene delivery to spinal cord motor neurons using *in vitro* and *in vivo* assays.
3. **EVALUATE THE EFFICACY OF CANDIDATE TRANSGENES AND MOTOR NEURON TROPISM IN ANIMAL MODELS OF SPASTICITY.**
   Severity of spasticity will be evaluated in animals that have undergone spinal cord injection of viral vectors carrying antispasticity transgenes; Glutamate decarboxylase (GAD) and TeTxLC.
   a. Evaluate the effect of sciatic nerve injections of rAAVGAD and rAAVTeTxLC on the spastic mouse model of spasticity using behavioral and anatomical assays.
   b. Evaluate the effect of sciatic nerve injections of rAAVGAD and rAAVTeTxLC on spinal cord contusion induced spasticity in Sprague-Dawley rats using behavioral and electrophysiological assays.

c. Construct and assay the activity of targeted rAAV for the delivery of antispasticity genes.

b. Background and Significance

Background for Gene Transfer to the Nervous System

Several vector systems have been used for gene transfer *in vivo* including adenovirus, herpes simplex virus (HSV), rAAV and lentiviruses. The existence of standard techniques for gene insertion and deletion (10) allows for viral attenuation preventing vector replication, as well as the addition of potentially therapeutic genes. Vectors constructed with adenovirus (11), HSV (12, 13), AAV (14), and lentivirus (15) can effectively transduce neurons, suggesting these vectors may be applied to the treatment of neurological disorders.

Adenovirus

To date, most work in the nervous system has been performed with adenoviruses. Davidson and coworkers utilized an adenoviral vector carrying the hypoxanthine-guanine phosphoribosyltransferase (HGPRT) gene to correct enzyme deficits in a mouse model of Lesch-Nyhan syndrome (16). Adenoviral vectors have been used to deliver neurotrophic factors to motor neurons. Using an axotomy model for progressive motor neuron loss, two groups successfully attenuated cell loss with BDNF, CNTF, and GDNF. In each case the growth factors were delivered to the injured motor neurons via retrograde transport following an intramuscular injection of the appropriate adenoviral vector (17, 18).

We have reported adenoviral gene transfer to motor neurons via direct injection into the spinal cord (6, 19) or via retrograde transport (20, 21). One limitation of adenoviral vectors in our own work (6, 19-21) and that of others (14, 16) is the three week time course of expression. The termination of adenoviral gene expression may depend on cytolytic or noncytolytic mechanisms. Cytolytic termination of gene expression could result from direct viral toxicity (22) or the action of immune mediators (23). The immune response to viral vectors is biphasic with an early response to the viral capsid proteins. This phase of the reaction involves activation of microglia, $CD4^+$ T cells, and macrophages (24). In a later phase of the inflammatory response, $CD8^+$ T cells respond to viral proteins presented to MHC class I molecules in transduced neural cells (26). Remote delivery is likely to limit the early phase of the inflammatory response in the CNS by eliminating viral capsid proteins from this region. However, leaky expression of viral proteins, even from replication-defective vectors, could still trigger a late phase CD8+ response resulting in neural cell death. Nonetheless, our laboratory has documented motor neuron survival following *in vivo* gene transfer in the remote delivery paradigm (27). This finding suggests that a noncytolytic mechanism is responsible for the termination of gene expression. Because immunosuppression prolongs gene expression, we suspect that inflammatory cytokines terminate gene expression at the level of promoter regulation.

The recent work of Lowenstein and colleagues suggests that the early stage of immune response to CNS injection of first generation adenoviral vectors is limited in duration and functionally insignificant. The later stage of inflammatory response within the nervous system only occurs when the immune system has been sensitized to adenoviral gene products through expression in non-CNS environments. Thus, prolonged expression of first generation adenoviral transgenes is possible if vector administration can be confined to the CNS. Advanced generation adenoviral "gutted" vectors do not appear susceptible to this peripheral sensitization dependent shutdown. This finding suggests that leaky expression of viral genes is responsible for the termination of CNS expression in first generation vectors (Lowenstein, personal communication). The difficulty in achieving prolonged CNS expression with first generation has motivated us to develop advanced generation vector strategies for motor neuron gene delivery.

Adeno-associated Virus (AAV)

Unlike lenti and herpes based vector systems, AAV is a parvovirus that has not been linked to any human pathological processes (28). The AAV capsid has no envelope and is 20-25 nm in diameter. It contains a 4680 base single stranded DNA genome (29). The viral genome integrates into host cell chromosomes. The AAV genome has been detected as a single integrated copy in two experiments (30, 31). Nonetheless, multiple copy integration has been demonstrated and some authors suggest that the genome can exist in host cells without integration (32). The integrated AAV remains in a latent state until the host cell is infected with either an adenoviral or herpes helper virus. The presence of genes from the helper virus allows wildtype AAV to enter a lytic cycle (33).

rAAV vectors contain only 4% of the wild-type genome. The remaining DNA consists of the inverted terminal repeat sequences (ITRs) at the 5' and 3' ends (34). The native DNA encodes seven genes in 2 open reading frames, including 3 *cap* structural proteins, and 4 *rep* proteins. In order to create rAAV, one must transfect cells with an AAV packaging plasmid containing rep and cap in the absence of ITRs and an AAV

vector plasmid containing the expression cassette cloned between ITRs. The remaining genes necessary to trigger a lytic cycle can either be provided by a helper virus or an adenoviral helper plasmid. The latter contains the VA, E2A, and E4 genes under the control of their adenoviral promoters (35).

rAAV can infect a broad range of cells in multiple species including human, non-human primate, canine, murine, and avian cells. It can transduce both dividing and non-dividing cells. This latter characteristic lends rAAV to application in the CNS. rAAV can selectively transduce neurons (36) with gene expression in the spinal cord present up to one year following direct injection of type 2 rAAV(37). Duration of gene expression can vary depending on the promoter utilized and the specific neuroanatomic location of delivery. Klein noted an early loss of expression in the hippocampus of rats injected with a CMV driven rAAV transgene (38). Mandel and colleagues showed that fusion of the CMV promoter with the human beta-globin promoter prevented early shutdown of gene expression, allowing expression beyond one year (39). The neuron specific enolase (NSE) promoter provides a means of targeting gene expression to neurons with gene expression observed 19 months after injection (38). With the NSE promoter, neuronal gene expression is present in different types of neurons including GABAergic, cholinergic, and dopaminergic cells (38). In parallel, application of the myelin basic protein promoter enhances gene expression in the white matter above the levels seen with CMV, NSE, or GFAP promoters (14).

Of the 6 serotypes of AAV, the application of AAV2 to the nervous system has been studied in the greatest depth. AAV2 appears to be taken up selectively by neurons (our preliminary and proposed experiments utilize AAV2, see Preliminary Data Figs. 11-15, 18). In non-neuronal *in vitro* systems, AAV2's uptake depends on binding to heparin sulfate proteoglycans (40). Our own data (see Preliminary Data) and that of others suggest that CNS injection of AAV2 has no deleterious effects on tissue. Chamberlin and colleagues were unable to detect microglial infiltrates or gliosis in transgene expressing tissue (41). In a series of behavioral experiments, amphetamine caused similar locomotor effects and stereotyped behaviors in rats following AAV versus control substantia nigra injections (14).

The absence of destructive effects on tissue has laid the groundwork for the therapeutic use of AAV in the nervous system (3). For example, 2 approaches are currently being used for the treatment of Parkinson's disease. The first approach involves rAAV-mediated delivery of critical enzymes in the dopamine synthetic pathway including tyrosine hydroxylase, GTP cyclohydrase, and aromatic amino acid decarboxylase while the second approach involves the delivery of neurotrophic growth factors aimed at preventing nigral degeneration (3). rAAV has also been applied to other models of CNS injury. Mandel (42) demonstrated that the delivery of NGF and BDNF with rAAV2 injected into the basal forebrain prevents the loss of cholinergic neurons induced by fornix lesions. Similarly, the delivery of BDNF to the spinal cord using rAAV protects rubrospinal neurons from atrophying following spinal cord injury (43). Alternatively, the rAAV-mediated delivery of antisense sequence has the capacity to reduce expression of genes and alter neural functional properties. Xiao reports that the expression of antisense sequence of the alpha 1 subunit of the GABA receptor in the inferior colliculus reduces GABA ligand binding and increases seizure activity (44).

AAV Configured for Selective Motor Neuron Uptake

Recently several investigators have made progress in understanding the mechanism underlying the native tropism of the 6 AAV serotypes. The capsid of AAV derives from 3 *cap* genes that encode structural proteins VP1, VP2, and VP3. The C-terminal regions of these proteins end in a beta barrel conformation and constitute the protein coat of the virus. The loop structures and N terminus of the virus plays a role in the interaction of the capsid with the internal viral DNA and the external environment (45). VP1 and VP2 make up 5% of the capsid while VP3 makes up the remaining 90% (46).

The current application proposes experiments aimed at studying manipulation of the rAAV coat in order to enhance the vector's CNS tropism. There are 6 sites capable of accepting foreign epitopes or ligands that might alter viral tropism without affecting DNA packaging or infectivity (9). These sites include the N terminus of VP1 near aa34, the N terminus of VP2 near aa138, the loop I region (aa266), the loop IV region (aa447 or 591), or the loop V region (aa664). The tissue tropism of AAV can be targeted by attaching peptides at these sites. Wu and colleagues inserted the serpin ligand at the N terminus of VP1 and VP2. Lung epithelia, which express the serpin receptor, were infected by the targeted virus containing the serpin ligand. Infectivity increased 62 fold over cells infected with wild-type AAV (9). In parallel, Bartlett and colleagues utilized a bispecific antibody recognizing both the megakaryocyte-specific cell surface receptor integrin and the AAV capsid to increase the ability of AAV to infect CD34 megakaryocytes (47). Girod cloned the L14 ligand known to bind to several integrins into the six loops of the *cap* proteins. Three of these mutants expressed L14 on their surface and one was noted to infect AAV resistant cells (48). Thus, the groundwork has been laid for targeted AAV delivery.

Two strategies exist to target rAAV gene delivery to motor neurons,. The first attempts to link neurotropic proteins to VP capsid protein external residues. The second is to create a series of chimeric viruses expressing small neurotropic peptides on the viral capsid. The first strategy has the disadvantage of requiring the production of chimeric antibodies (Ab) to the surface of rAAV and an extra step in the production of rAAV for application. Nonetheless, this strategy allows for the use of relatively large ligands without concern for the kinetics of DNA packaging. Similar chimeric monoclonal Abs have been created for the targeting of adenoviral vectors (49). In this strategy, monoclonal Fab fragments are covalently linked to a ligand for which there is a known receptor. Rogers and colleagues have exploited this approach to target adenoviral vectors carrying oncolytic transgenes to tumors expressing receptors for the growth factors (50, 51).

Two candidate proteins exist for the production of chimeric monoclonal Abs. The first is the rabies G protein, which is 505 amino acids (AA) in length and is 50 kDa in size. The rabies virus is an enveloped, nonsegmented, RNA rhabdovirus. The virus penetrates the nervous system through uptake into PNS terminals and retrograde axonal transport (52). Initial viral replication occurs in primary sensory and motor neurons. The rabies virus expresses one protein on its lipid envelope that is thought to mediate viral tropism via specific binding to cell surface receptors. This protein is known as the G glycoprotein. G glycoprotein is approximately 500 amino acids (aa) integral transmembrane protein (53). The external domain contains two immunodominant conformational sites: site II and site III (54, 55). Site III is necessary for membrane penetration and neuronal specificity. This site spans aa 330-338. Lysine 330 and Arginine 333 of G glycoprotein are basic residues that play an important role in binding to the acidic p75-NTR protein (56). Homology between G glycoprotein and α-bungarotoxin and d-tubocurarine suggest that the nicotinic acetylcholine receptor also plays a role in rabies uptake (57). NCAM may be another cell surface receptor that bind the G glycoprotein (53). Our strategy to develop a G glycoprotein-containing AAV vector is discussed in the Methods section of this proposal.

The second protein fragment that has documented motor neuron tropism is the C-fragment of BoNT which is a 41 kDa fragment of the 900 kDa holotoxin (58). The sequences of the holotoxins for the genes of the various BoNT serotypes are well documented. The C-fragment of BoNT varies throughout the 7 serotypes of botulinum with 35% sequence homology between some types (59). The major receptor for these molecules are surface gangliosides, G_{T1b} and G_{Q1b}, and show selective binding to motor neurons in spinal cord explant cultures(60).

The construction of rAAV viruses that express small neurotropic peptides on their capsid surface may be superior to the first strategy as it eliminates the step of producing chimeric monoclonal Abs. Since the production of rAAV requires separate transfection of viral packaging cell lines with a helper plasmid (pXX2 or pIM29-45) and a shuttle plasmid carrying the expression cassette, production of mutant pIM29-45 with insertion of small neurotropic peptides would allow for flexibility in packaging various neurotherapeutic transgenes. Muzycka and colleagues have shown that peptides ranging from 5-10 AA in length can be inserted into the cap gene to create mutant pIM29-45 that remain capable of packaging viral DNA and maintain infectivity (9).

We have identified several candidate short peptides with inherent neurotropism. The first peptide group are snake venom neurotoxins. Toxins from the family Elapidae (cobras, kraits, mambas) and Hydrophidae (sea snakes) bind the acetylcholine receptors (AchR) with high affinity. These toxins have a high degree of sequence homology with the rabies G protein. Short toxins ranging from 60 to 62 aa in length are the focus of our investigation (57). A second group of neurotropic peptides have been identified in the toxins of scorpions and sea snails. These toxins bind to neuronal ion channels including the voltage gated Na+ channel and K+ channel. They are both approximately 30 aa in length (61, 62).

Short peptide neurotransmitters represent a third group of potentially neurotropic peptides. These neurotransmitters exist throughout the nervous system and are distributed in a system specific fashion (63). Thus, rAAV expressing short neurotransmitter peptides may be capable of utilizing the synaptic machinery for peptide neurotransmission to bind target neurons. Calcitonin Gene Related Peptide (CGRP) is present in up to 90% of spinal LMNs (64). CGRP is 37 aa in length. Lastly, the neurotropism of coronavirus responsible for a variety of encephalitic conditions is thought to derive from a decapeptide sequence expressed between two coiled-coil sequences on the surface of the coronavirus (65). These latter candidate peptides could be utilized in the event that toxin based approaches alter DNA packaging or fail to provide adequate motor neuron uptake.

Construction of the targeted rAAV vector and other vectors is supported by the University of Michigan Gene Therapy Center Vector Core. Success in vector construction with the Gene Therapy Center is well documented by our publications (6, 7, 66) and Preliminary Data.

Spasticity Overview

Lance (67) describes spasticity as a motor disorder characterized by a velocity-dependent increase in muscle tone (tonic stretch reflexes). Minor spasticity can cause pain and disability, while severe spasticity can result in musculoskeletal deformity. The broad impact of spasticity derives from its association with multiple disease processes. Spasticity occurs most frequently in cerebral palsy, multiple sclerosis, stroke, spinal cord injury, and head trauma (68).

Studies conducted by Sherrington on decerebrate cats created a framework for understanding the neurophysiology underlying spasticity in the late 19th century that allowed for the development of surgical and pharmacologic treatments of the syndrome (69). Sherrington demonstrated that the loss of upper motor neuron input to spinal and brainstem reflexes resulted in a state of disinhibition.

Because of its simplicity both the neuroanatomy and physiology of the spinal reflex arc are well understood. This understanding has defined possible sites for the pathophysiology of spasticity. The reflex control of motor function depends on multiple sensory inputs, multiple synaptic mechanisms, and multiple motor outputs. Regulation of muscle tone depends on input from muscle spindle organs that detect change in *muscle length* and Golgi tendon organs that detect *muscle tension* (70, 71). The primary sensory neurons transducing these signals reside in the dorsal root ganglion (DRG) and project to lower motor neurons (LMNs) through mono- and polysynaptic connections. Polysynaptic connections involving inhibitory spinal interneurons allow for the creation of reciprocal inhibition, wherein antagonistic muscle groups are prevented from simultaneous contraction. Thus, spindle associated sensory fibers simultaneously stimulate motor neurons capable of initiating a reflex contraction that resists the muscle stretch, and inhibit the motor neurons of muscles that might prevent that contraction. In contrast, golgi associated fibers project entirely to motor neurons through inhibitory interneurons resulting in an inhibition of contraction in the muscle under tension (72). Importantly, inhibitory interneurons may act through either presynaptic or postsynaptic inhibition.

Two forms of motor neurons receive golgi and spindle input; α and γ cells. α-motorneurons project to extrafusal muscle and control the neuromuscular connection to the majority of striated muscle. γ-motorneurons innervate intrafusal muscle fibers within the muscle spindle and control the organ's sensitivity by adjusting the tension and hence sensitivity of the fibers within the spindle (73).

Thus, there are a limited number of sites within the reflex arc where spasticity might occur. First, spindle associate afferents may lose either presynaptic inhibition or reciprocal inhibition. Alternatively, golgi associated inhibitory activity may be reduced. Alterations in spinal interneuron activity may also result in spasticity. For example, loss of activity in the Renshaw interneurons thought to mediate reciprocal inhibition can trigger spasticity. Finally, increased motor output in either α or γ neurons can trigger spasticity (74). While increased γ motor output has historically been thought to be responsible for spasticity, evidence exists to support a multifactorial mechanism (75).

The balance of these mechanisms determines the resting tone of muscle, as well as its response to passive and active movement. Supraspinal input from upper motor neurons (UMNs) controls this important balance. It is likely that the corticospinal tract cooperates with both the reticulospinal and vestibulospinal tracts to govern muscle tone. The corticospinal tract stimulates both α-motorneurons as well as inhibitory interneurons. The dorsolateral reticulospinal tract is, itself, largely inhibitory. Thus, damage to the dorsal spinal cord damaging both corticospinal and dorsolateral reticulospinal pathways profoundly shifts the balance of motor tone by eliminating inhibition (76,73, 77).

Finally, spasticity is not the result of an immediate alteration in the balance of supraspinal control of spinal reflex arcs (77). The development of spasticity is often preceded by a phase of spinal shock during which muscles are areflexic and lack tone. The clinical presentation of spasticity may occur weeks after the insult that triggered it (78). Various mechanisms may contribute to the timing of onset of spasticity. Dietz (78) postulates that spinal shock may involve a reversible reduction in activity of the α or γ motorneurons during the period that immediately follows loss of supraspinal input. Thus, the delayed onset of spasticity may reflect the gradual resolution of spinal shock. In contrast, evidence exists for the gradual development of GABA receptor supersensitivity following loss of supraspinal input suggesting a progressive loss of inhibition (79).

Treatment of Spasticity

The pain, functional deficits, and secondary musculoskeletal deformities caused by spasticity are all indications for treatment. Chronic pain can result from flexor spasms in the affected limbs. Patients with preserved limb function may experience improved ambulation and arm function with alleviation of spasticity. In nonambulatory patients, profound spasticity can create difficulties with nursing care including difficulty with patient hygiene as well as bed to chair and bed to bed transfers. Finally, chronic spasticity may result in an exacerbation in decubitus ulcers and tendon contractures.

The simplicity of the spinal reflex arc has allowed for the development of multiple therapies, though each of these carries inherent disadvantages. Current therapies of spasticity include pharmacological and surgical interventions, physiotherapy, and implantable drug delivery systems. Drugs targeting the GABA system, baclofen and diazepam, constitute the majority of pharmacological therapy for spasticity. The second class of antispasticity agents are adrenergic including Tizanidine and clonidine. The application of both adrenergic and GABAergic antispasticity drugs is limited by general CNS depression, and may be complicated by liver toxicity.

Botulinum toxin (type-A) represents an alternative approach to the treatment of spasticity. Clostridial neurotoxins (CNTs) are zinc proteases that act by disabling the intracellular machinery for synaptic vesicle binding necessary for the release of neurotransmitters. The toxins are translated as a single 150 kDa polypeptide chain that is cleaved into a light and heavy chain linked by a disulfide bond. The heavy chain is responsible for neurospecificity and membrane translocation. Botulinum toxin (BoNT) is highly specific for cholinergic LMNs, while tetanus toxin (TeTx) is specific for inhibitory spinal interneurons. The light chain is responsible for catalytic cleavage of a protein component of the SNARE complex responsible for synaptic vesicle docking in the axon terminal. Currently, BoNT-A is approved by the FDA for use in the treatment of strabismus, blepharospasm, and hemifacial spasm. Nonetheless, the toxin is being used off-label for multiple conditions including spasticity. The use of BoNT is limited by the need for repeated dosing due to the transience of the toxin's effect. Cholinergic synaptic function recovers when the protein toxin has been metabolized and new SNARE complexes are synthesized. The formation of antibodies to the BoNT can limit the use of repeated injections. Diffusion of BoNT to neighboring muscles may result in weakness in muscles not targeted. In the case of strabismus, this effect may result in transient ptosis (80).

Surgical treatment of spasticity has focused on ablation of various components of the spinal reflex arc and may be conducted on the spinal cord itself or the peripheral nervous system. These procedures either interrupt the afferent side of the spinal reflex arc, as in the case of selective dorsal rhizotomy, or damage the peripheral nerve, as in the case of radiofrequency rhizotomy. While these procedures provide treatment options for patients with refractory spasticity, they all rely on destruction of neural structures in order to be successful (68). The implantation of intrathecal pumps for the delivery of baclofen provides an alternative to ablative procedures. Since FDA approval in 1992, 11,000 baclofen pumps have been implanted (Medtronic personal communication). The application of pumps has been limited by the high (33%) incidence of hardware related complications, anatomical limitation to the lumbar spinal cord, and high maintenance (68). Thus, all current therapies of spasticity bear significant limitations.

Why Attempt Gene Therapy of Spasticity?

For the purposes of the current proposal, spasticity provides a model system in which to develop strategies for neuronal targeting of gene based synaptic inhibition. The relative functional simplicity of the spinal reflex arc provides an excellent mammalian model for interrogating the mechanisms of gene based neuromodulation. However, gene therapy possesses inherent advantages for clinical application to spasticity.

While a variety of pharmacological and surgical approaches to spasticity exist, each carries associated complications and side effects. Adeno-associated viral gene therapy has the potential to create a long-lasting motor neuron-specific attenuation in spasticity without ablating neural structures. All of the currently existing pharmacological treatments for spasticity with the exception of BoNT-A lack anatomic specificity, and are therefore limited by CNS depression. Surgical approaches with the exception of intrathecal pumps are ablative. These approaches carry the risk of weakness and sensory loss and are inherently irreversible. Current neurosurgical interventions with reversible effects carry the inherent disadvantages of implantable devices enumerated above. BoNT has provided a strategy for the treatment of spasticity that is motorneuron specific and nonablative. However, the need for repeated administration of an immunogenic protein has limited its utility.

Viral gene transfer into the spinal cord represents an alternative approach with the ability to manipulate the machinery of neural transmission in selected target cell types without altering anatomy or damaging neural tissue. Furthermore, inducible promoters create the potential for controlled production of transgenes. As discussed above, intraparenchymal injections of adenovirus, herpes, rAAV, and lentiviral vectors result in gene product expression in both neurons and glia (6, 40, 81-83). The limited time course of transgene expression by early generation adenoviral and herpes vectors as well as the inflammatory response to viral expression restricts application of these vectors to human disease (6, 84). Nonetheless, the inflammatory response to CNS viral gene delivery may be eliminated by preventing antigen presentation outside the nervous system (27, 85). In addition, application of advanced generation vector systems including lentivirus, rAAV, and gutted adenovirus have the potential to substantially prolong gene expression in the nervous system without inducing

inflammatory damage (86, 87). Also, importantly the combination of advanced generation vector systems with controllable promoter systems creates the potential for long term regulated gene delivery in the CNS. Kafri et al (88) have demonstrated high efficiency control of gfp expression in the brains of immunocompetent rats using the Tet-induceable system.

Remote injection of viral vectors into the PNS or adjacent tissue for selective transport into the CNS represents a minimally invasive alternative to direct spinal cord injection (7, 66). This approach affords many advantages: cell selectivity, decreased inflammation, absence of direct injections into an already compromised CNS and easy accessibility. In addition, motor neuron specificity and axonal uptake can be enhanced by targeting the vector capsid. As discussed, a variety of targeting strategies exist including covalently modifying a vector capsid (49), altering the capsular genes of a vector (48), and pseudotyping membrane encapsulated vectors (83). Both remote delivery and motor neuron vector targeting are relatively unexplored and the focus of the current application.

Animal Models of Spasticity

The study of human spasticity benefits from an array of animal models for spasticity. The majority of animal experiments on the physiology of spasticity have focused on traumatic models of decerebration and spinal cord injury. However, both inflammatory and genetic models of spasticity exist. The optimal application of antispasticity gene therapy to multiple sclerosis, cerebral palsy, spinal cord injury, and brain injury patients may require variations in vector and transgene selection. Models vary in preparatory difficulty, as well as appropriate assays for spasticity. Genetic models can be easily bred or purchased, while traumatic models must be surgically induced. However, the latter model provides the advantage of behavioral and electrophysiologic analysis of spasticity in a larger animal preparation.

Several feline and rodent models of traumatic spasticity have been explored. Traumatic spasticity models differ in the level at which the lesion is made, the type of lesion made, and the species in which the model is applied. The majority of traumatic spasticity models have been conducted in cats. In these animals, decerebration can be performed via a stereotactic disconnection of descending tracts with a precollicular incision that separates the midbrain from the diencephalon (89). Alternatively, lesions can be made in the cervical, thoracic (90), and lumbar (91) spinal cord. Spinal cord injuries for the purpose of studying spasticity have largely been incomplete. Injuries can be induced by microsurgical sectioning of selected quadrants of the spinal cord (92), or can be induced by graded weight drop contusion models (93). In some cases, spinal cord ischemia induced either by aortic cross clamp (94) or intraaortic balloon inflation (95) has been used to induce spasticity. None of the animal models of spasticity are absolutely precise in the degree of spasticity generated. However, traumatic models do allow for a grading in the severity of spasticity. The degree of injury induced by a weight drop model can be reliably adjusted by changing the force transduced into the spinal cord (93). Likewise, microsurgical resection of spinal cord tracts can be graded. However, the consistency of injury severity in these models will vary significantly with the skill of the surgeon inducing the lesion. In particular, damage to cord vascular structures can result in exaggerated effects of tractotomy models. Urinary retention represents a significant disadvantage of chronic spinal cord injury models (96). These animals require manual bladder evacuation two to three times per day. Attempts to eliminate urinary retention have been made by targeting lesions to the sacrocaudal region of the spinal cord, but this model limits the study of spasticity to tail motor function (97).

Spasticity can be modeled in animals that carry mutations of inhibitory amino acid receptors. The spastic mouse mutations result in behavioral abnormalities resembling sublethal poisoning with the glycine antagonist, strychnine. Insertion of a LINE-1 element into the gene for the β subunit, Glrb creates the spastic phenotype (98). The insertion causes aberrant splicing in the β receptor unit (99). The $Glrb^{spa}$, spastic homozygotes show spastic symptoms which can occur spontaneously but can be induced reliably by handling at approximately 14 days of life. The spasms consist of rapid tremor, stiffness of posture, and difficulty in righting (100). No anatomical pathology occurs in either muscle or central nervous system of spastic mice, except that herniated intervertebral discs and cysts of the leptomeninges have been noted (101). The spastic symptoms can be reduced with intraperitoneal injection of an inhibitor of GABA transaminase (102). These animals express less than 20% the normal density of glycine receptors (103). A genetic model of spasticity exists in Han-Wistar rats, although the exact nature of this mutation is unknown. Expression of RNA isolated from the cerebellum of these spastic rats creates abnormally high glutamate sensitivity in a Xenopus oocyte assay, suggesting that these animals may suffer from enhanced glutamate sensitivity (104).

Finally, spasticity can be modeled with both toxic and inflammatory insults. The spasticity that results in multiple sclerosis can be modeled with chronic relapsing experimental allergic encephalitis (CREAE) in the mouse (105) or in the rat (106). Antispasticity effects of pharmacological agents have been studied in the

Biozzi ABH (antibody high) mouse model (107). In this model, sensitization with spinal cord homogenate in adjuvant results in a chronic relapsing pattern of disease. Finally, spastic myelopathy has been induced in rabbits using intraperitoneal and intracisternal injection of a neurotoxic plasticizer, N-butyl benzenesulfonamide (108).

We propose to screen our antispasticity vectors in the spastic mouse model because of its convenience. We will study the mechanism vector action in the traumatic thoracic spinal cord model, which provides graded levels of injury in a rat model amenable to easy behavioral and physiologic analysis.

Assays for Spasticity

Spasticity can be quantified through anatomical, behavioral, and electrophysiologic assays. Behavioral examination depends on a blinded examiner grading a single response or group of responses. Some investigators have utilized the regularity of spastic extension in response to abdominal stimulation on repeated trials (109). Other investigators have used composite scales in which individual observations of multiple parameters including deep tendon reflexes, righting reflex, myoclonus, urinary retention, clonus, and limb hypertonia are summated (108). Alternatively, the degree of spasticity can be scored at hip, knee, and ankle on a 0-5 scale (110).

Ossowska and colleagues describe force transducer measurements of rat ankle dorsiflexion and plantar flexion. These measurements show increased muscle tone in response to haloperidol treatment (111) and advanced age (112). Similarly, the mean force required to flex hindlimbs on repeated trials can be measured as an assay of spasticity in order to test the effects of antispasticity pharmacological agents (107). Elevations of the "Dynamic Force Amplitude" measured as resistance of the ankle to dorsiflexion during movement are sustained up to 66 weeks following lower thoracic spinal cord injuries (92).

A limited number of histological and anatomical measurements may reflect chronic spasticity. Cosgrove and Graham (113) have reported consistent shortening of the gastrocnemius length and lengthening of Achilles tendon lengths in spastic mice when compared to phenotypically normal litter mates. These changes in length provide an assay for the contractures experienced by children with cerebral palsy and can be prevented with BoNT-A injection. Ziv et al (114) reported reduced numbers of sarcomeres and a reduced rate of muscle growth in spastic mice.

EMG measures of spasticity have utilized chronically indwelling hindlimb electrodes in the soleus and gastrocnemius muscles. Peak EMG amplitudes measured from these electrodes during foot dorsiflexion (Dynamic Amplitude) are demonstrated to increase by 40% following thoracic spinal cord injury (92). Alternatively, monosynaptic reflexes (MSR) can be quantified in flexor and extensor muscles by recordings from peripheral nerves following stimulation of dorsal roots. These roots are divided distally to the stimulating electrode in order to prevent antidromic action potentials from passing into the peripheral nerve. In hemisected animals, spasticity is reflected by an increased ratio of the MSR on the injured side to the MSR on the intact side in comparison to control animals. Likewise, the mean MSR in both flexor and extensor nerves is elevated in injured animals as compared to control animals (91).

Summary

In summary, this proposal seeks to develop strategies for motor neuron specific gene delivery and strategies for targeted neuromodulation through localized inhibition of synaptic function. We have selected spasticity as a clinical model because improved treatment of this disorder will depend on targeted, nondestructive, controllable neuromodulation. In addition, the simplicity of the spinal reflex arc will facilitate a better understanding of targeted gene based neuromodulation.

Our team of investigators is in a unique position to accomplish this goal. The award applicant, Dr. Boulis, has accepted a faculty position in the Department of Neurosurgery at the Cleveland Clinic Foundation. *This department has made restorative neurosurgery and neuromodulation a clinical priority (see Appendix).* The development of targeted synaptic inhibition will be applicable to stereotactic neuromodulation in the treatment of Parkinson's disease, epilepsy, eating disorders, and pain.

In parallel to his appointment at the Cleveland Clinic, Dr. Boulis will maintain his affiliation with the newly established Program for Understanding Neurological Diseases (PFUND) funded through industrial and philanthropic support. The PFUND is pursuing a parallel line of research into targeted motor neuron gene delivery for application to motor neuron disease (ALS). In addition to Dr. Boulis, the senior members of PFUND including a senior ALS neurologist/neuroscientist, and 2 research scientists expert in the analysis of mouse tissues and in vitro neuronal assay systems will focus their efforts on this proposal. As outlined in our publications (in the Appendix (6, 7, 66) and in the Preliminary Data) the required viral vectors and the surgical and anatomical expertise to complete the experiments in this proposal are present in our group. Importantly,

construction of the viral vectors will be funded in part by the PFUND. To facilitate multi-investigator use of our data, our results will be posted on our web site, www.pfund.umich.edu quarterly. We encourage the reviewers to go to our web site if time permits. In parallel with the proposed study, an endowment to the PFUND is supporting AAV viral vector development of therapeutic proteins (IGF-I, BDNF, GDNF). *This parallel approach of characterizing gene delivery to motor neurons for the dual targets of neurodegenerative and functional disease will shorten the time necessary to develop human therapies and augment Dr. Boulis' resources.*

c. **Preliminary Data**

Dr. Boulis has conducted extensive studies of the delivery of genes to the spinal cord, vector design, and gene based neuromodulation laying the foundation for the current proposal.

Direct Viral Gene Injections into Spinal Cord

Preliminary experiments demonstrated our ability to successfully transfer adenoviral vectors directly into the normal adult rat spinal cord (6, 7, 66). The adenoviral vector for delivery of the gene for β-galactosidase (Ad5RSVLacZ) was directly injected into adult Sprague Dawley rat thoracic spinal cord. LacZ expression is present in both white and gray matter over an approximate 1.2 cm length amounting to almost 20% of the total cord. The time course of LacZ gene expression (β-galactosidase staining) over 21 d reveals peak expression at 7 d post injection (Fig. 1). Histological examination of these spinal cords revealed gene expression in neural, glial, and endothelial cells with significant inflammatory response (Fig. 2).

Fig. 1. 3 mm Sections of Rat Spinal Cord Stained Following Direct Intraparenchymal Ad5RSVLacZ Injection. Spinal cord adenoviral gene expression peaks 7 d following Ad5RSVLacZ intraparenchymal injection.

Fig. 2. Microhistology Following Direct Intraparenchymal Ad5RSVLacZ Injection. A. Glial cell staining. B. Endothelial staining. C. Sensory neuron staining. D. Intermediolateral nucleus staining. E. Dural staining. F. No ependymal staining

Remote Viral Gene Delivery After Sciatic Nerve Injection

Targeted delivery of viral gene products to the spinal cord using remote injection may prolong gene expression and decrease the inflammatory response. To test this hypothesis, sciatic nerves were injected with Ad5RSVLacZ and analyzed for β-galactosidase staining. Sciatic nerve injection resulted in viral gene expression

Fig. 3. Remote Injection Model Delivery System. The sciatic nerve of animals are injected with virus. The virus is transported to the spinal cord. A) The sciatic nerve injection site. B) Dorsal root ganglia. C) Dorsal horn of the spinal cord. D) Ventral horn of the spinal cord.

in spinal cord neurons (Fig. 4A). β-galactosidase staining in the sciatic nerve injection site existed predominantly in perineurium, but not within the nerve's axons (Fig. 4B). Staining was seen in both the sensory neurons of the dorsal root ganglia as well as the sensory neurons of the dorsal horn. However, staining in the lumbar spinal cord was seen predominantly in ventral horn cells with the morphologic characteristics of motor neurons (Fig. 4C and D). The ipsilateral motor neurons are likely to project directly into the sciatic nerve (Fig. 4D). However, staining was unexpectedly detected in the motor neurons of the contralateral side, which are unlikely to project into the sciatic injection site (Fig. 4C). Both surgical division of the nerve and intraneural colchicine injections blocks all spinal cord uptake suggesting that gene expression is due to retrograde transport of Ad5RSVLacZ to the spinal cord. To clarify the significance of bilateral gene expression in the ventral horn after unilateral injection, the sciatic nerve was co-injected with the retrograde tracer, Fluoro-

Gold. Comparison of the number of neurons staining was discreetly confined to the ipsilateral ventral horn while β-galactosidase gene expression was seen in all quadrants. The largest quantity of β-galactosidase positive neurons was noted in the ipsilateral ventral horn (Fig. 5A). Because Fluoro-Gold labels only first order neurons projecting directly into the sciatic nerve (Fig. 5B), the finding of β-galactosidase expression in all quadrants suggests that the viral transgene is delivered to sec

Fig. 4. Expression of β-galactosidase 7 d Following Sciatic Nerve Injection of Ad.RSVntLacZ. A. Composite of the lumbar spinal cord showing neuronal gene expression bilaterally. B. Perineurial β-galactosidase in the sciatic nerve injection site. C. Contralateral neuronal viral gene expression in the ventral horn. D. Ipsilateral neuronal gene expression.

Fig. 5. Spinal Cord Viral Gene Expression has a Distinct Pattern of Distribution in Comparison with that of Fluoro-Gold. A. Fluoro-Gold is detected only in the ipsilateral ventral horn, while β-galactosidase expression following Ad.RSVntLacZ injection into the sciatic nerve occurs in all four quadrants. B. Fluoro-Gold signal detected in the ipsilateral ventral horn.

Remote Viral Gene Delivery: Injection Survey, Time Course and Dose Response

Preliminary experiments surveyed the uptake and retrograde transport of vectors after injection into subcutaneous tissue, muscle and nerve. β-galactosidase gene expression in spinal cord following injection of 2 λ
Ad5RSVLacZ into crushed or uncrushed sciatic nerve was compared with gene expression following injection of 50 λ into either the anterior tibialis muscle or the subcutaneous space of the footpad (Fig. 6). ANOVA revealed a significant group effect ($p < 0.05$). Subanalysis revealed significantly higher gene delivery by crushed or uncrushed sciatic nerve injection than either subcutaneous or intramuscular injections.

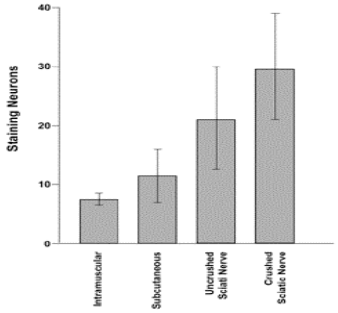

Fig. 6. Gene Delivery Following Sciatic Nerve, Muscle or Footpad Injection. 1.8×10^7 pfu Ad5RSVLacZ injected into the sciatic nerve results in more spinal cord gene expression than 4.5×10^8 pfu injected into either muscle or the footpad (ANOVA: $p < 0.05$, subanalysis reveals nerve to exceed muscle and footpad).

Furthermore, this increased effect in nerve is achieved with only 4% of the volume and viral titer required
for subcutaneous or muscle injections. Subanalysis did not reveal a difference between injection into crushed and uncrushed sciatic nerves.

Next, the time course of remote gene expression was characterized after sciatic nerve injection. All animals underwent right sciatic nerve injection with 1.8×10^7 pfu Ad5RSVLacZ. Spinal cords were harvested at 30 min, 3 d, 6 d, 12 d, or 18 d following viral injection (Fig. 7). ANOVA revealed a significant effect of

interval between injection and harvest ($p < 0.005$). The analysis revealed a significant increase in gene expression between 30 min and 6 d, as well as a significant reduction in gene expression between 6 d and 12 and 18 d.

Viral titer significantly affects the number of cells stained via remote gene delivery. The number of neurons staining increased between the doses 1.8×10^6 pfu and 1.8×10^7 pfu ($p < 0.03$). However, this effect

Fig. 7. Time Course of Spinal Cord Gene Expression Following Sciatic Nerve Viral Injection. Gene expression can be detected as early as 30 min following injection, but peaks at 6 d. (ANOVA: $p < 0.005$, subanalysis reveals significant differences between 30 min and 6 d, and between 6 d and 12 or 18 d)

Fig. 8. Viral Titer Alters Gene Delivery. Increased gene expression can be detected between 1.8×10^6 pfu and 1.8×10^7 pfu, but not at higher doses (ANOVA: $p < 0.05$, subanalysis reveals an increase between 1.8×10^6 pfu and 1.8×10^7 pfu, but not 1.8×10^7 pfu and 4.5×10^7 pfu).

appeared to plateau at higher doses with no further increase in neuronal staining observed at titers of 4.5×10^7 pfu (Fig. 8).

Immunosuppression Augments Viral Gene Expression

Immunosuppression can augment viral gene expression. Rats implanted with sustained release 7.5 mg dexamethasone tablets for 3 weeks had significantly more neuronal staining in both lumbar spinal cord and dorsal root ganglion neurons following sciatic nerve injection. The number of cells staining for β-galactosidase was significantly greater 12 d following injection suggesting that gene expression is prolonged by dexamethasone administration ($p < 0.0001$). Importantly, the number of lumbar motor neurons staining in immunosuppressed animals is greater than the number of motor neurons staining at the peak dose and peak time point (6 d) in untreated animals. Amplification has also been observed following treatment with cyclosporine.

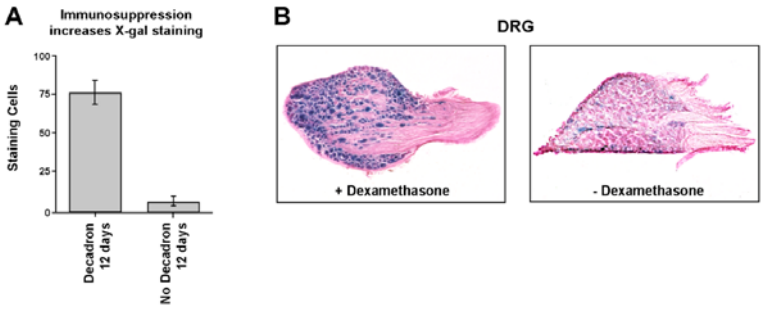

Fig. 9. Dexamethasone Increases Spinal Cord Viral Gene Expression. Remote (sciatic nerve) gene delivery in rats is augmented by treatment with subcutaneous administration of sustained release dexamethasone.

To determine whether the reduction in number of β-galactosidase staining cells over time results from the death of neurons expressing β-galactosidase, DNA fragmentation was assayed in nonimmunosuppressed animals as an indication of cell death. An ANOVA comparing virus and saline treated animals shows no sig

Fig. 10. A. Sciatic Nerve Injection with Ad5RSVLacZ vs. Saline induces niether DNA fragmentation nor reduced neuronal density. TUNEL ($p = 0.989$, $n = 40$). Neuronal Density ($p = 0.913$, $n = 40$).

difference in the number of cells with fragmented DNA ($p = 0.989$, $n = 40$) (Fig. 10A). The cell death detected by TUNEL staining in both groups occurred universally in non-neuronal cells with no detection of motor neuron cell death. In addition to an absence of DNA fragmentation, microscopic histological analysis revealed no evidence for the cellular swelling associated with necrotic cell death. TUNEL staining was present in all positive control spinal cord tissue treated with DNase prior to the assay.

Motor neuron densities in the ventral horn of the spinal cords from virus and saline treated animals were also calculated by dividing the number of cresyl violet stained neurons (Fig. 10B) in the spinal cord ventral horn by the area of this region. An ANOVA comparing motor neuron densities in control and infected animals at all time points revealed no significant group effect ($p = .913$, $n = 40$) (Fig. 9), indicating that virus infection does not reduce motor neuron density.

AAV Provides Prolonged Gene Expression

AAV induces a reduced host immune response compared to adenovirus. To compare adenoviral with AAV viral remote delivery, either Ad5RSVLacZ or AAV vectors with the Rous sarcoma virus (RSV) promoter and the reporter genes for lacZ (AAVRSVLacZ) or GFP (green fluorescent protein, AAVEGFP) were injected into the sciatic nerve.

Five ul of AAVRSVLacZ (viral titer 1.4×10^7 particles/ml) and Ad5RSVLacZ (viral titer 1.4×10^7 pfu/ml) were microinjected into the right sciatic nerve of adult rats ($n = 5$ for each group). After 21 d, animals were sacrificed and the tissue was stained for β-galactosidase expression. While remote delivery of Ad5RSVLacZ stained a limited number of neurons after 21 d (Fig. 11A), abundant neuronal staining was present after AAVRSVLacZ injection (Fig. 11B, C). Positively stained lumbar neurons in both groups were quantified. Sciatic nerve AAV injections resulted in significantly higher viral expression than the adenoviral control group ($p < 0.05$, $n = 10$) (Fig. 12). Similarly, animals injected with AAVGFP had abundant GFP expression in the neurons of the dorsal root ganglia and in lumbar spinal cord motor neurons after 21 d which was absent in controls (Figs. 13, 14). Collectively, these data suggest that remote intraneural AAV injection represents a potential method to prolong gene expression in the spinal cord.

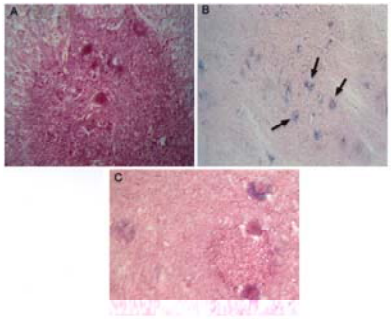

Fig. 11. 21Day Ad vs. AAV A) Remote AdRSVLacZ (10^6 pt) B&C) Remote AAVRSVLacZ (10^6 pt).

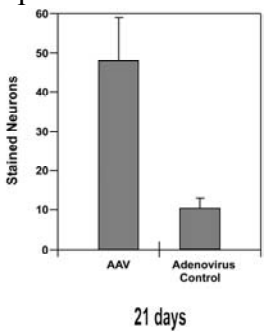

Fig. 12. Remote Injection of AAVRSVlacZ (1.4×10^4 pt /ul) and AdRSVlacZ (10^4 pfu/ul) ($p < 0.024$).

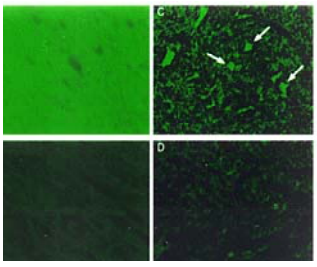

Fig. 13. A) Sciatic nerve injected with AAVEGFP B) Sciatic nerve injected with AAVRSVLacZ C) GFP expressing lumbar neurons following Remote injection with AAVEGFP D) No GFP expressing neurons following remote injection with AAVRSVLacZ

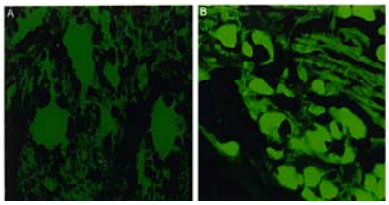

Fig. 14. A) GFP expressed in motor neurons of the spinal cord remotely injected with AAVEGFP (40 x). B) GFP expression in the DRG of animals injected with AAVEGFP (40 x)

Remote Delivery to High Cervical Spinal Cord and Brainstem Motor Neurons

One of the chief limitations of current treatments of spasticity is the difficulty with treatment of the upper extremities. We have perfected the surgical techniques necessary to deliver viral vectors via direct nerve injection into the laryngeal nerve and high brachial plexus. To expose the recurrent laryngeal nerve, a horizontal incision is made on the ventral surface of the rat neck, between the angle of the mandible and the sternal notch. The incision is carried through skin and platysma. Skin and platysmal flaps are elevated superiorly and inferiorly. The fascia encompassing the submandibular salivary glands is divided in the midline. The strap muscles are divided in the midline to expose the larynx and trachea. The recurrent laryngeal nerves

may be visualized on the lateral aspects of the trachea bilaterally, within the tracheoesophageal groove. The left recurrent laryngeal nerve is dissected superiorly and inferiorly. (Fig. 15). For exposure of the mouse brachial plexus, a longitudinal incision is made through the skin just ventral to the axilla. Superficial fat and fascia are pulled inferiorly to expose the lateral edge of the pectoralis major muscle. The lateral edge of the pectoral muscle is gently elevated to reveal the brachial plexus. The brachial plexus is dissected superomedially and inferolaterally (Fig. 16).

We have successfully injected the mouse brachial plexus with rAAVEGFP (5 λ of 1.4 x 10^7 particles /ml, n = 5). After 21 d, animals were sacrificed and the brachial plexus, cervical cord and brainstem were processed for GFP expression. There is abundant GFP fluorescence in neurons from both the high cervical cord. and brainstem. These data suggest that remote intraneural AAV injection represents a potential method to deliver therapeutic proteins into the high cervical cord and brainstem.

Fig. 15 **Fig. 16**

Stereotactic Neuromodulation with rAAVGAD

Chemical, mechanical, and electrolytic lesions of the lateral hypothalamus as well as single unit recordings implicate the lateral hypothalamus in the control of eating (115). GABA and GAD are localized to the hypothalamic regions implicated in the control of feeding (116). Further, GABA antagonists injected into the lateral nucleus of the hypothalamus (LH) cause increased food intake suggesting that GABA may play a role in the inhibition of feeding (117). Further, rAAV vectors capable of producing GAD, the enzyme responsible for GABA synthesis, has been developed (118). We therefore undertook to examine the feeding behavior of Wistar rats following LH stereotactic delivery of rAAVGAD. Fig. 17 demonstrates the distribution of GFP in the LH following injection of 500 nl of rAAVGFP (10^4 pt/λ). Fig 18 depicts the change in food consumption in rats following injection with either saline, rAAVGFP, or rAAVGAD at the same titer. Augmentation of AAVGAD in the LH, causes a reduction in food intake, while saline and control vector injected animals show the expected increase in food consumption (119).

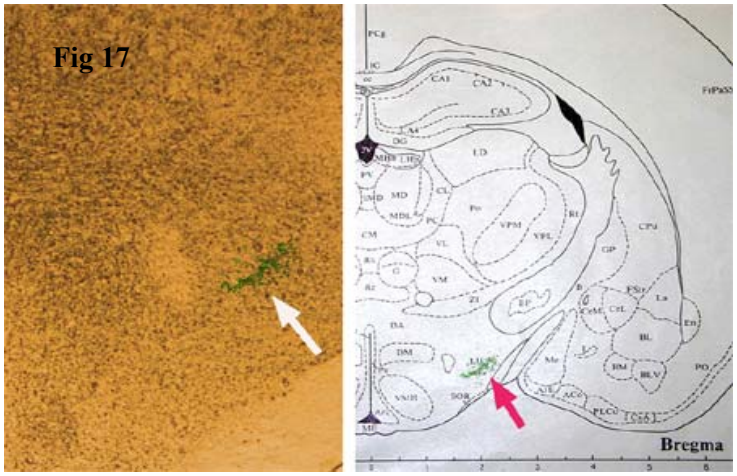

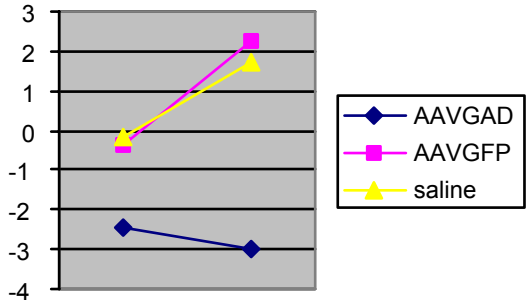

Fig. 18. Change in food consumption depicted in daily grams. Hypo-thalamic GAD expression reduces food intake.

In Vitro Motor Neuron Growth

In order to develop neurotropic mutants of rAAV, an *in vitro* assay for motor neuron viral gene transduction is necessary. Our laboratory has successfully demonstrated survival of motor neurons in culture. Spinal cords are harvested from E15 animals and dissociated under sterile conditions. These cells are cultured in L-15 supplemented with albumin, catalase, SOD, transferrin, galactose, progesterone, putrescine, selenium, estradiol, hydrocortisone and antibiotics. Robust motor neuron survival is confirmed with islet-1 immunohistochemical staining up to 14 days after culturing (Fig. 19). Further, we have successfully transduced these cells in culture with adenoviral vectors. This system provides an *in vitro* assay system for screening uptake and expression of viral transgenes delivered with targeted vector systems.

Spinal Cord Injury Model

Based on design parameters received from Jean R Wrathall at Georgetown University, we constructed a weight drop spinal cord contusion apparatus in the University of Michigan Machine Shop (Fig. 20). This design was used in preliminary experiments to confirm consistent results with those presented by Gale et al (93). These animals demonstrate almost complete recovery of locomotor function at 2.5 cm but persistent deficits at a 5 cm weight drop. Persistent spasticity is noted in both groups.

Fig. 19: Dissociated E15 spinal cord in vitro. Islet-1 stain labeling demonstrates motor neuron enrichment (70%).

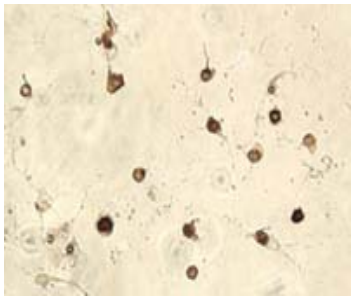

Fig. 20 Spinal cord impounder apparatus for delivery of reproducible graded spinal cord injuries

Vector Design

In collaboration with the laboratory of Michael Imperiale and the Vector Core at the University of Michigan, we have constructed a series of adenoviral and rAAV vectors. Initial first generation adenoviral vectors were constructed by cloning cDNA for the growth factor IGF-I (obtained from the laboratory of Peter Rotwein; pBKIGF-1) into the shuttle vector system pAdRSV4loxp (obtained from the laboratory of Gary Nabel) between the RSV promoter and SV40 poly adenylation sequence. This shuttle system contains the first 16 m.u. of the serotype 5 adenoviral genome (Ad5) with a deletion of the E1a and E1b sequence. The RSV promoter, a polycloning site, and the SV40 polyA sequence are inserted into this deletion. This shuttle system, pAdRSVIGF-Iloxp, contains the loxp sequence cloned at the 9.2 m.u. site. Separately, cSub360loxp (a cosmid containing the loxp sequence followed by the 9.2 to 100 m.u. of Ad5 containing a deletion of the E3 gene: obtained from GaryNabel) was linearized by restriction digest. Finally, an *in vitro* recombination of pAdRSVIGF-1loxp and cSub360loxp was performed using the Cre recombinase to yield AdRSVIGF-Iloxp. Conditioned media from 293 cells infected with AdRSVIGF-Iloxp was screened in a IGF-I receptor tyrosine phosphorylation assay demonstrating the production of active IGF-I (Fig. 21).

Fig. 21: Bioactive IGF-I produced by Ad.RSVIGF-Iloxp

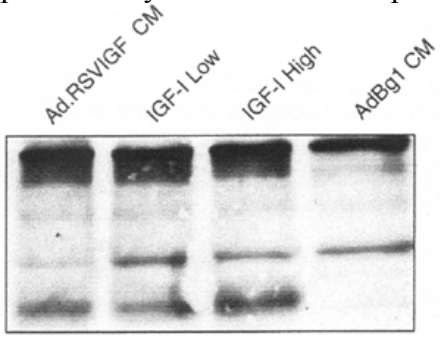

Subsequent to the production of AdRSVIGF-Iloxp, we have constructed the recombinant adeno-associated viruses AAV-CMV-*IGF-I*, AAV-CMV-*GFP*, and AAV-CMV-*IGF-I*-IRES-*GFP*. The rat IGF-IA cDNA was excised from the plasmid pBK-*IGF-I* and cloned into the AAV transfer plasmid pSUB201 (gift of R.J. Samulski, Gene Therapy Center Vector Core, University of North Carolina). The final AAV vector plasmid contained a CMV promoter, the rat IGF-IA cDNA, simian virus 40 (SV40) polyadenylation sequence, and flanking inverted terminal repeat sequences (ITRs). A corresponding AAV vector plasmid was constructed using the cDNA for the green fluorescent protein (GFP). Recombinant AAV-*IGF-I* and AAV-*GFP* viral particles were produced by cotransfecting the respective AAV vector plasmid with the helper plasmid pXX2 into 293 cells. The plasmid pXX2 contains the rep and cap genes from the AAV serotype 2 genome. The 293 cells were infected with wildtype adenovirus 5 at a multiplicity of infection of 2. Two days post-adenovirus infection, the cells were harvested and freeze/thawed. Recombinant AAV particles were separated from adenoviral particles using cesium chloride density centrifugation. The AAV band was collected, dialyzed against DMEM, and heated at 56 degrees Celsius for 30 minutes to inactivate any trace amounts of wildype adenovirus. An additional recombinant AAV vector, AAV-CMV-IGF-I-IRES-GFP, was prepared from the AAV vector plasmid pTRUF5 (gift of Nicholas Muzyczka, University of Florida) that was subsequently designed to contain the CMV promoter, rat IGF-IA cDNA, an internal ribosome entry site (IRES) sequence, the GFP sequence, and an SV40 polyadenylation signal, all collectively flanked by ITRs. The IRES-GFP sequence was originally contained within the plasmid MSCV2.2 (Erle Robertson, University of Michigan).

Summary

These preliminary data establish our ability to evaluate all aspects of direct and remote viral vector delivery to both rats and mice. Our group is unique in our capacity to fully characterize remote and direct viral delivery to spinal cord and brainstem. Further, we have demonstrated the ability to produce adenoviral

vectors capable of producing bioactive neurotherapeutic transgenes. We have developed a dissociated motor neuron culture system necessary for the in vitro examination of motor neuron targeting. Finally, we have demonstrated that rAAVGAD can be used to affect gene based neuromodulation.

c. **Research Design and Methods: EXPERIMENTAL APPROACH**

1. CONSTRUCT NOVEL ANTISPASTICITY VECTORS TO DELIVER THE LIGHT CHAIN (LC) OF TETANUS TOXIN (TeTx).

The light chain of TeTx has been shown to selectively block neural transmission via intracellular protease activity. The absence of the associated heavy chain prevents this transgene from producing an active neurotoxin.

a. Produce first generation adenovirus (Ad.RSVTeTxLC) containing an expression cassette of the 1.9 kb TeTx LC under the control of the rous sarcoma virus (RSV) promoter by Cre-Lox *in vitro* recombination.

Rationale: In aim #1, we attempt first to create an adenoviral vector expressing the TeTxLC, demonstrate its ability to create bioactive TeTxLC *in vitro*, and its ability to inhibit motor neuron function *in vivo*. If the first stages of this aim are successful, we will construct a shuttle plasmid for the creation of rAAVRSVTeTxLC. The toxicity of the TeTxLC gene expression will be evaluated at each stage of development.

As discussed in the Background and Significance section of this application, TeTx holotoxin contains a heavy and light chain. The heavy chain is necessary for neuronal specificity, cellular binding, and membrane translocation of the catalytic light chain. Poulain et al (120) and others have demonstrated that TeTxLC is not toxic when applied to the extracellular surface of neurons. When injected into the cytoplasm of neurons, the light chain is capable of inducing a highly efficient blockade of neural transmission that lasts until new SNARE proteins can be synthesized. The light chain is not toxic to the metabolism of neurons or other cell types. The use of a viral vector to induce the intracellular synthesis of TeTxLC should be capable of abolishing synaptic transmission in all neurons infected by the virus for the duration of gene expression even at low levels of gene expression.

Experimental Design: Plasmid DNA containing the gene encoding for TeTx will be extracted from C. tetani strain Y-IV-3 (WS 15). PCR primers for the ends of the sequence for TeTxLC (residues 1-457 of the holotoxin) as well as a carboxy terminal truncated L chain (TeTxLCct: residues 1-427), and an amino terminal truncated L chain (TeTxLCnt: residues 30-457) will be synthesized. The carboxy terminal truncated L chain is reported to have increased activity while the amino truncated L chain should have significantly attenuated activity (121).

TeTxLC:
5'end: 5'-AGCGGATCCCCAGGAATGCCAATAACCATAAATAATTTTAGATATAGTGATCCTGT-3'
3'end: 5'-TGCGAATTCTTATGCAGTTCTATTATATAAATTTTCTCTTATATTTGTTGGTGG-3'
TeTxLCct
5'end: same as TeTxLC
3'end: 5'-AGCGAATTCTTAATCAACATTTCTAAAAGCATTTGTATTTACCCTCATATTTTG-3'
TeTxLCnt
5'end: 5'-CGGCACTATCCAAATACGATCTGTTATTTTGAAGGCCTTATAATAGCTATC-3'
3'end: same as TeTxLC

These, PCR primers will be designed to include appropriate polylinker sequence for subsequent cloning efforts with the resulting fragments. TeTxLC, TeTxLCct, and TeTxLCnt will each be cloned into pAdRSV4loxp to create individual shuttle vectors for each fragment. pAdRSV4loxP contains the first mapping unit (m.u.) of the wildtype Ad5 genome followed by the RSV promoter, a multicloning site, and the SV40 polyadenylation sequence, and lastly the loxP sequence. By cloning the LC fragments into the multicloning site, three shuttle vectors pAdRSVTeTxLC, pAdRSVTeTxLCct, and pAdRSVTeTxLCnt are created. In each case, the LC expression cassette, containing the promoter, 1371 bp LC sequence or 1281 bp truncated LC sequence, and the polyadenylation sequence, replaces the E1a and E1b region of the Ad5 genome.

The cosmid cSub360loxP contains the loxP sequence followed by the 9.2-100 m.u. of the Ad5 genome with a deletion of the E3 region. Because the cosmid does not contain the inverted terminal repeat (ITR) or packaging sequence it cannot be replicated or packaged by itself, eliminating the possibility of contamination of the recombinant virus with wildtype sub360 virus. The loxP and viral sequence are removed with a Cla I

digest. Separate *in vitro* recombinations will be conducted between the individual LC shuttle vectors and the linearized viral sequence from the cSub360 using Cre recombinase (Fig. 22).

To produce recombinant adenovirus, 5 µg. of Cre treated DNA is transfected into 60 mm dishes of 293 cells. These cells express the E1 region deleted from the recombinant viruses. When cytopathic effect is noted

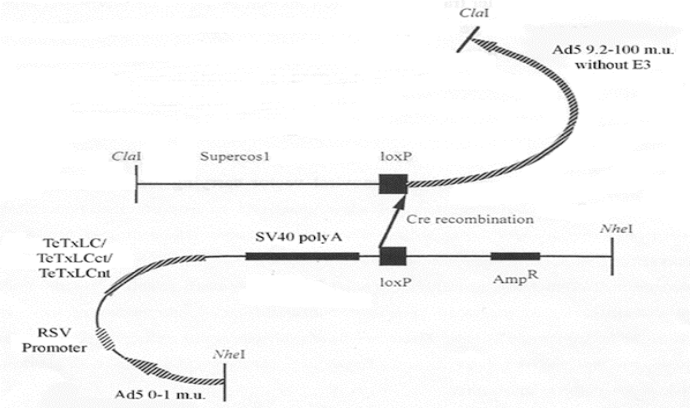

Fig. 22: In Vitro Cre-LoxP Recombination. The 3' end of adenovirus sub360 is excised from the cosmid cSub360 and recombined in vitro with the 5' end of Ad5 containing the novel antispasticity expression cassette. Cre recombinase recognizes the loxP sequence *in vitro*.

in the 293 cells (7-9 days), a crude lysate is made from the cells. This lysate is then used to infect a 100mm dish of 293 cells. Crude lysates of the recombinant viruses AdRSVTeTxLC, AdRSVTeTxLCct, and AdRSVTeTxLCnt will be doubly plaque purified. PCR will be used to confirm insertion of the fragments in the virus. These vectors will be amplified and purified using the University of Michigan Vector Core facility. The plasmid DNA necessary for construction of adenoviral vectors has been obtained from the University of Michigan Vector Core and the laboratory of Gary Nabel. The sequence for TeNTLC will be obtained by PCR using published primer sequences (121).

Anticipated Results: We anticipate the production of three first generation adenoviral vectors for the delivery of two potentially active TeTxLC fragments and one inactive TeTxLC. Given our previous success at constructing first generation adenoviral vectors using the Cre-Lox *in vitro* recombination system (See Preliminary data: Fig. 20), we do not foresee any difficulty with vector construction. Appropriate precaution will be taken in the handling of the clostridium used for PCR isolation of the TeTx fragments.

One conceivable concern about the production of AdTeTxLC is the potential for inadvertent human inoculation of respiratory epithelium. Appropriate respiratory isolation procedures will be utilized in the handling of these vectors. As discussed, tetanus light chain is not inherently dangerous because it lacks the heavy chain necessary for neuronal delivery. However, because the virus is designed to deliver the LC to cells, the virus is expected to be capable of inhibiting synaptic function. Nonetheless, CNS delivery of adenoviral genes has never been documented following transduction of respiratory epithelium. The blood brain barrier prevents significant penetration of the nervous system following intravenous delivery (122) even following intracarotid infusion of $5x10^{11}$ pt.s of Ad.RSVlacZ.

The substrate for the TeTxLC Zn protease is the vessicle associated membrane protein (VAMP) of the synaptic vessicle binding complex (SNARE). The family of VAMP proteins are located in a variety of nonneuronal tissues including the endocrine system, liver, and kidney (123). The VAMP proteins play a role in exocytosis in these tissues. Thus, the inadvertent gene delivery of TeTxLC to tissues other than the nervous system would carry the potential risk of a disruption in secretory function in the location inoculated. Intravenous delivery delivers virus predominantly to the liver. Thus, high titer intravenous inoculation would pose a risk to liver function. In addition, pulmonary inoculation would carry the risk of temporary reduction in the production of pulmonary secretions For this reason, live virus will be evaluated for toxicity in rats prior to proceeding with functional assays (see aim 1c).

b. Assay for TeTxLC activity in neuronal (SH-SY5Y cells) and nonneuronal cell lines (3T3 cells) infected with Ad.RSVTeTxLCs using a rapid fluorescence based assay.

Rationale: We plan to assay both neuronal and nonneuronal cell lines for TeTxLC activity in order to determine if the TeTxLC vectors and control vectors induce the production of bioactive light chain catalytic activity. Aim 1b is designed to compare the activity of TeTxLC, TeTxLCct, and TeTxLCnt present in concentrated conditioned media as well as the cellular fraction. Aim 1b will also test for cellular toxicity of the vectors in neuronal and nonneuronal cell lines.

Experimental Design: 3T3 fibroblasts and SHSY5Y neurablastoma cells will be cultured to 70% confluence in DMEM with 10% fetal calf serum (FCS) in P60 at 37 degrees in a humidified atmosphere with 10% CO_2(124).

Cells will be obtained from the laboratory of Eva Feldman MD., PhD. Dishes will be exposed to 5 m.o.i. of virus for 30 min then incubated for 48 hrs. Media is harvested and concentrated with centriprep 30 centrifugal concentration filters (Amicon). Cells are scraped from the culture dish and exposed to a lysis buffer. Protein is harvested and the concentration is determined and normalized.

Using the assay described by Soleilhac et al (125) protein from the cellular fraction and conditioned media is assayed for TeTxLC proteolytic activity. Briefly, the assay depends on synthesizing a 50-mer synaptobrevin peptide (S39-88) with a fluorescent phenylalanine residue substituted for the tyrosine at the end of the peptide. This peptide will be synthesized at the University of Michigan Peptide Core facility. Protein from the cellular and conditioned media fractions will be suspended in 20 mM Hepes at pH 7.4. The protein will be brought to a concentration of 500 ng per 80 □. 20 □ of the synthetic peptide will then be added to the LC solutions or a control solution containing no active protein. The reaction will be kept at 37 degrees for 30 min in the dark, then stopped with 0.9 ml of 72% MeOH with 0.1% TFA. The 1 ml. mixture is then loaded on a Sep-Pak Vac C_{18} cartridge (Waters) containing 500mg of C18 reverse phase. These cartridges are pre-equilibrated with 10 ml. of 65% MeOH with 0.1% TFA. This same solution was used to elute 3 ml after the first 1 ml. is taken off. The relative fluorescence at 343 nm and 377 nm is measured for the eluant on a spectrophotometer. The concentration of S77-88, one of two metabolites created by TeTxLC activity, is estimated by the amount of fluorescence in the separated fraction.

In order to estimate the effect of the LC vectors on cell survival, 60 mm dishes of 3T3 cells and SHSY5Y cells will be exposed to the individual vectors; AdRSVTeTxLC, AdRSVTeTxLCct, AdRSVTeTxLCnt, AdRSVlacZ at an m.o.i. of 5 or an equal volume of vehicle. Cell survival will be determined by photographing the dishes at 24 hrs, 72 hrs, and 1 week.

Anticipated Results and Potential Problems: We anticipate that AdTeTxLC and AdTeTxLCct will generate intracellular TeTxLC activity but not AdTeTxLCnt. We expect AdTeTxLC to infect 3T3 cells at approximately the same rate as SHSY5Y cells since first generation adenovirus are capable of infecting both fibroblasts and neurons. We anticipate that cell survival will not be affected by viral infection at 5 m.o.i. In the event that no TeTxLC activity is detected, monoclonal antibodies to TeTxLC will be used to perform western blot analysis on the various fractions to determine whether the viral transgene is being expressed and is not bioactive or is not being adequately expressed. Given that the TeTxLC and TeTxLCct have previously been cloned and expressed
and shown to be bioactive (121), we do not expect either expression or bioactivity to present a problem.

c. Evaluate hindlimb motor function of rats following lumbar spinal cord and sciatic nerve Ad.RSVTeTxLC injection for proof of principle and evaluate the potential for pulmonary or hepatic toxicity.

Rationale: This aim attempts to demonstrate that *in vivo* delivery of the TeTxLC gene is capable of reversibly inhibiting LMN function. While first generation adenovirus is unlikely to prove useful in the treatment of spasticity due to its limited duration of expression, proinflammatory features, and the resistance of the nervous system to adenoviral reinjection (66). Our work has previously demonstrated spread of first generation adenoviral gene expression up to 6 mm from the injection site lasting up to 3 weeks following injection (6). This aim will also attempt to demonstrate that TeTxLC expression in the lumbar spinal cord does not induce respiratory depression. Separately, the effect of intravenous and endotracheal administration of AdRSVTeTxLc on liver and pulmonary function will be evaluated.

Experimental Design: Sprague-Dawley rats (n=5) will undergo injection of 4 □ of either TeTxLC or TeTxLCct, depending on which virus showed greater activity in the *in vitro* assay. Two control groups (n=5 per group) will undergo injection with AdRSVlacZ or AdRSVTeTxLCnt. Two viral titers, 10^8 and 10^6 pfu, will be evaluated for each group.

Anesthesia and Monitoring: Sprague-Dawley rats (350g) will be induced under either pentobarbital or isofluorane anesthesia. Mice (30g) will be anesthetized with isofluorane anesthesia only. Isofluorane anesthesia is induced by placing animals in a chamber that is connected to the isofluorane ventilation system. Rats undergo endotracheal intubation once asleep, and receive an isofluorane/oxygen mixture for the remainder of the procedure (for dosing see below). During all procedures a rectal temperature probe is used to maintain body temperature at 37.5 degrees Celsius. Ventilated is maintained with a Harvard Rat Ventilator. Rats are intubated with angiocatheters under direct visualization using an operating microscope.

Direct Spinal Cord Injection: Using sterile technique, the paraspinous muscles of the L3 region are elevated from the lamina and spinous processes. A hemilaminectomy is performed using cuticle scissors at the midthoracic level. A micromanipulator is then used to insert a glass capillary tube beveled to 50 microns in

diameter into the spinal cord at the midline. 4 λ of viral solution is delivered using a nanoject oocyte injector apparatus. Paraspinous muscle is sutured and the skin is stapled.
Incline Plane Assay: Rats are placed head down on an adjustable inclined plane that is covered with a rubber mat (126). The incline is increased from 0 degrees until the rat cannot maintain its position for greater than 5 sec. This incline decreases with increased severity of sensorimotor dysfunction.
Animals will be assayed for hindlimb motor function using an incline plane assay described above. The AdRSVlacZ group will be sacrificed on day 7. Spinal cords will be processed and the area of βGalactosidase staining will be quantified to determine the volume of cord transduced.
Quantification of Gene Expression Within Spinal Cord: In order to quantify and compare remote delivery of vectors to the spinal cord, spinal cord neurons expressing GFP are quantified. Animals are sacrificed 21 days after viral injection. Following intracardiac perfusion with buffered 4% paraformaldehyde, the lumbar spinal cord, sciatic nerve, and lumbar dorsal root ganglia (DRGs), high cervical cord, and brainstem are removed and tissue is postfixed in 2% paraformaldehyde at 0°C for 4 h and blocked. For β-galactosidase, tissue is rinsed 3 times in lacZ rinse (2 mM $MgCl_2$, 0.1 mg/ml Na deoxycholate, 1/5000x Triton-X in PBS), then 3 times in PBS at 0°C for 5 min each and incubated in X-gal stain (Invitrogen kit, Carlsbad, CA) for 12 h at 37°C. Tissue is rinsed 3 times in PBS at 0°C for 5 min each and immersed in 2% paraformaldehyde at 4°C for 4 h and in PBS with 20% sucrose at 4°C until negatively buoyant. Tissue is then frozen in optimal cutting temperature gel (OCT, Sakura Finetek Inc, Torrance, CA) and cryosectioned. 35 μ sections of spinal cord are taken from each block of stained tissue. Tissue sections will be digitally photographed and the area of tissue staining with β-galactosidase will be quantified with NIH image software.

The remaining groups will be followed with serial incline plane measurements for 2 months to assess deterioration and recovery of hindlimb function. At 2 months, the AdRSVTeTxLC and AdRSVTeTxLCnt groups will be sacrificed and the spinal cords will be removed. Cresyl violet staining will be done in order to calculate the mean motor neuron density of the lumbar spinal cord to evaluate whether motor neuron death has occurred in the experimental group. A control group (n=5) of sham operated animals will also be sacrificed at 2 months to serve as a control group for the purpose of lumbar motor neuron density.

Separate groups of animals will undergo spinal cord, subcutaneous and endotracheal injection with 4 □ of 108 pfu's of the AdRSVTeTxLC or AdRSVlacZ. Animals will be observed for respiratory dysfunction and tail vein blood will be tested every 3 days to liver enzymes to establish whether liver or lung toxicity is induced in experimental animals as a result of extra-CNS VAMP degradation.
Anticipated Results: We expect that animals treated with AdTeTxLC will develop the gradual onset of hindlimb flaccid weakness that will be longer lasting and more significant in the higher titer group. Animals that receive either AdRSVlacZ or AdRSVTeTxLCnt are not expected to show signs of motor dysfunction. We do not anticipate respiratory compromise in any group. Nonetheless, animals will be examined twice daily to ensure that no urinary retention is caused by viral gene expression and that no signs of dyspnea are noted. Animals showing signs of respiratory difficulty will be euthanized. Motor neuron density measurements are anticipated to show some reduced cell numbers in all viral treated groups in comparison to the sham operation group, given the inflammatory response that we have previously observed in the spinal cords of animals directly injected with first generation adenoviral vectors (6). These experiments will serve as proof of principle that neuromuscular function can be inhibited in a viral titer dependent fashion without motor neuron toxicity.

Given the lack of targeting in the direct injection paradigm of first generation adenoviral systems, the specificity of AdRSVTeTxLC's action will be limited. It is anticipated that all spinal neurons infected will undergo a temporary synaptic blockade. While we anticipate flaccid weakness and numbness to be the result of this nonspecific blockade, it is possible that the animals will develop pain or dysregulation of motor function. All behavioral observations in this case will be valuable. However, animals will be euthanized for any sign of persistent discomfort.

Given the widespread distribution of VAMP in secretory tissues of the body, the potential for nonspecific toxicity exists. We do not anticipate significant alteration of liver function with any route of administration since the LC transgene is unlikely to be delivered to a sufficient percentage of hepatic cells without a direct portal vein injection. The activity of TeTxLC in alveolar tissue has not previously been tested. Different isoforms of VAMP have varied sensitivity to TeTxLC, and therefore the effect of endotracheal administration of AdRSVTeTxLC is unknown (127). We suspect, however, that this form of administration will create severe atelectasis as a result of reduced surfactant production. This finding will help to guide the appropriate safety procedures necessary for viral handling.

d. Construct a rAAV vector for the delivery of TeTxLC (rAAVRSVTeTxLC).

Rationale: If the TeTxLC transgene proves capable of transiently inhibiting synaptic function in the rat hindlimbs, we will proceed to construct a rAAVCMVTeTxLC. This vector will be constructed for use in Aim 3, in order to test the efficacy of this novel approach to eliminating spasticity.

The production of rAAV depends on the cotransfection of packaging cells with a plasmid vector containing the ITRs of AAV flanking an expression cassette (pTRUF-5TeTxLC), and a separate vector containing the rep and cap genes of AAV (pXX2). Production of parvovirus requires the presence of genes from a helper virus. These can be supplied through coinfection of packaging cells with wild type adenovirus (Ad5), or by means of a helper plasmid containing the adenoviral genes required (pXX6).

Experimental Design: We will use the pTRUF-5 plasmid for the creation of rAAV. In order to make adequate room in the pTRUF-5 plasmid, the neo resistance sequence is removed by restriction digest. A separate restriction digestion is performed with Not I to remove the GFP sequence. The sequence of TeTxLC selected in aim 1b and tested in Aim 1c, will be cloned into pTRUF-5 between the Not I sites. Restriction mapping will be conducted to ensure the proper orientation of the transgene.

For harvesting virus, triple transfection will be conducted on 20 150 mm plates of 293 cells at 70-80% confluence. To make virus cells must be exposed to the proviral sequence, pXX2 carrying the rep and cap genes with no ITRs, and the pXX6 containing the adenoviral genes necessary for rAAV production. 25 μg. of plasmid DNA for pTRUF-5TeTxLC, pXX2, and pXX6 will be EtOH precipitated and resuspended individually in 18 ml of sterile water with 2 ml of 2.5 M $CaCl_2$. This solution is added to pH 7.05 0.05 M HEPES, 0.28 M NaCl, and 1.5 mM Na_2HPO_4 and 20 min later the mixture is observed for precipitation. 2 ml of each precipitate are added to each plate of cells. Cells are fed with Iscoves' modified eagles medium with 10% FBS and no antibiotics. The viral band will be isolated from the crude lysate by CsCl gradient ultracentrifugation and dialyzed into PBS with sucrose as a cryoprotectant. Viral titer will be estimated with slot blots.

Plasmids used for the construction of rAAV vectors have been supplied by the Jude Samulski, Ph.D. at the Center for Gene Therapy at the University of North Carolina (pXX2 and *pSub20*), and Nicholas Muzyczka of the Department of Molecular Genetics and Microbiology at the University of Florida Gainesville (pTRUF-5, pIM29-45, and pXX6).

Anticipated Results: We anticipate being able to clone the TeTxLC fragment into the pTRUF-5 plasmid without difficulty. Use of the helper-virus free system for rAAV production makes purification easier. However, to date, our ability to use helper-free systems for rAAV production successfully has been sporadic. In the event that we are unable to generate significant titers, we will revert to a wild type Ad5 helper system for rAAV production. This process requires both CsCl gradient purification as well as heat inactivation to avoid wild type Ad5 contamination.

2. DEVELOP STRATEGIES FOR TARGETED MOTOR NEURON DELIVERY OF rAAV ANTISPASTICITY TRANSGENES.

Enhanced neural uptake of rAAV-2 can be achieved through manipulation of the cap gene protein VP1.

a. Construct mutants of the rAAV cap gene in pIM29-45 by inserting candidate peptides at aa34 of the VP1 protein.

Rationale: Successful application of viral vectors to the problem of neuromodulation will depend on effective targeting strategies. The prevention of nonspecific effects depends on gene expression being confined to the systems under treatment and not bystander cells. By enhancing the neurotropism of rAAV vectors lower titers can be used in the remote injection paradigm hence reducing the potential for locally nonspecific effects. Targeting of this kind may be of particular importance if the TeTxLC vectors are found to have toxic effects in pulmonary tissue. Further, enhanced neurotropism may be essential for the delivery of genes to the compromised nervous system. In these instances, the normal mechanisms for axonal uptake and retrograde transport may be diminished. As such, targeted motor neuron delivery of rAAV may find application to Motor Neuron Disease as well as spasticity. The broader concepts may find application to engineered neurotropism for other CNS systems.

As discussed in the Background and Significance Section, there are two potential approaches to the construction of neurotropic rAAV. The first involves strategies for covalently binding neurotropic proteins to the surface of the rAAV capsid. This approach has the potential to permit the utilization of larger proteins like the rabies g protein or the Hc fragment of BoNT-A. This strategy requires the cumbersome extra step of capsid-tropic protein conjugation. We have therefore elected to pursue the second approach of constructing mutant rAAV capsids through the manipulation of the cap gene in pXX2/pIM29-45 plasmid. Construction of specifically neurotrophic pIM29-45 mutants will allow for the packaging of a range of rAAV2 shuttle vectors in viral coats with neuronal targeting. Because of the potential that longer insertions into the cap gene will alter

DNA packaging, we have chosen 60 AA short snake venom neurotoxin as well as the decapeptide of the neurotropic coronavirus to begin our investigation of engineered neurotropism.
Experimental Design: PCR primers are designed that contain codons for the 60 AA sequence of short snake venom neurotoxin (SSVN) or the decapeptide of coronavirus as well as a restriction site. This sequence is flanked by 20 bp on each side that are homologous to the parental plasmid pIM29-45. The resulting PCR fragments are digested with DpnI in order to eliminate parental plasmid DNA. These fragments are then cloned back into pIM29-45 for use in the production of rAAV. pIM29-45 functions like pXX2 to deliver the rep and cap genes for the packaging of vector DNA.
pIM29-45 containing the SSVN or decapeptide, are then used to created rAAV2 with pAAVGFP and helper plasmid pXX6 or wildtype Ad5 (as described in Aim 1d). The resulting rAAV2 is purified by CsCl gradient and heat inactivation. The resulting rAAVGFPdec or rAAVGFPssnt will be assayed for comparative infectivity *in vitro*, using 3T3 fibroblast and SHSY5Y cells.
Anticipated Results and Potential Problems: Aim 2a may not result in the production of viable rAAV. Previous attempts to alter the cap gene and hence create chimeric VP1 containing targeting surface proteins have used extremely short peptides ranging from 7-10 AAs. It is not clear whether larger proteins like SSNTs can be expressed as a part of VP1 without eliminating infectivity and DNA packaging. For this reason, we have included the decapeptide of coronavirus, which matches the length of insertions used in published experiments. However, this peptide may convey neurotropism without motor neuron specificity.

If mutation of the cap gene fails to produce a neurotropic rAAV packaging plasmid as tested in Aim 2b, we will defer to the alternative strategy of conjugated capsid proteins utilizing larger neurotropic proteins. This alternative approach is described below.
Conjugated rAAV capsid Targeting: The N-hydroxysuccinimide (NHS) derivative of phenylboronic acid (PBA) is conjugated to the Fab fragment of a monoclonal Ab which recognizes the surface moiety of the VP1 rAAV capsid protein (monoclonal core, Lerner Institute, Cleveland Clinic Foundation). In order to carry out this reaction, PBA NHS is dissolved in dimethylformamide (DMF) and added to Fab in PBS. The RV G protein and BoNT-Hc in 0.1 M $NaHCO_3$ are alkylated at cysteine residues with iodoacetimido dihydroxymethylbenzoate (DHBHA). PBA conjugated Fab readily binds to the DHBHA alkylation of the neurotropic proteins RV G and BoNT-Hc at room temperature. Targeted rAAV will be constructed in two steps. First, PBA anti-rAAV2 Fab will be bound to rAAV2GFP or rAAV2TeTxLC. Next, DHBHA RV G or DHBHA BoNT-Hc will be conjugated to PBA-Fab-rAAV2. The method proposed has been documented previously for the conjugation of Ad5 vectors to the FGF2 protein (49).

b. Evaluate the capacity of these strategies to enhance rAAV gene delivery to spinal cord motor neurons using *in vitro* and *in vivo* assays.

Rationale: Aim 2b attempts to determine whether the rAAV vectors produced in Aim 2a have an enhanced neural tropism for spinal motor neurons using *in vitro* and *in vivo* assays.
Experimental Design: Spinal cords are harvested from E15 animals and dissociated under sterile conditions. These cells are cultured in L-15 supplemented with albumin, catalase, SOD, transferrin, galactose, progesterone, putrescine, selenium, estradiol, hydrocortisone and antibiotics. Targeted rAAV will be exposed to dissociated embryonic spinal cord in culture. The levels of transgene expression in motor neurons elicited by targeted and untargeted vectors will be compared.

Groups of Sprague-Dawley rats will undergo sciatic nerve injection with either targeted rAAV2, and control rAAV2 containing expression cassettes for the GFP transgene. Control vector was obtained as a gift of Dr. Matthew During and Paola Leone of the Department of Neurosurgery, CNS Gene Therapy Center, Thomas Jefferson University. Amount of neurons transduced and the distribution of neurons transduced will be compared between systems using the histological method described in Aim 1 for examining spinal cord gene expression. Rather than quantifying the area of staining, as in direct spinal cord injection experiments, the number of neurons expressing GFP will be tabulated. For GFP quantification, tissue is visualized with fluorescence microscopy and fluorescent cells are counted. AntiGFP immunohistochemistry will be used to confirm the existence and distribution of viral transgenes in spinal cord. In remote delivery preparations, failure to detect transgene expression at the site of injection implies inadequate tissue injection or staining. Spinal cords from animals without injection site staining are therefore excluded.
Data Analysis: The mean number of spinal cord or brainstem cells staining in at least 10 selected sections are recorded for each animal and mean cell staining is then compared between groups using a single factor analysis of variance (ANOVA) for each experiment.
Anticipated Results and Potential Problems: We anticipate that rAAV2GFPdec will be capable of packaging DNA and maintaining infectivity. We predict that this vector will have enhanced transgene delivery to motor

neurons in culture and *in vivo* through remote delivery. Whether the targeted cap strategy will tolerate longer peptides like the SSNT is unknown. We suspect that if the vector is capable of packaging DNA, SSNT will convey a substantially higher neurotropism than the corona decapeptide. On the other hand, We hypothesize that conjugated vectors will deliver transgenes to motor neurons with substantially higher avidity *in vitro*. Nonetheless, because these vectors bear large potentially immunogenic antigens, they may not be tolerated *in vivo* due to proinflammatory responses. Animals will be monitored for such responses.

3. EVALUATE THE EFFICACY OF CANDIDATE TRANSGENES FOR INHIBITION OF SPASTICITY.

Severity of spasticity will be evaluated in animals that have undergone spinal cord injection of viral vectors carrying antispasticity transgenes; Glutamate decarboxylase (GAD) and TeTxLC.

A. Evaluate the effect of spinal cord injections of rAAVGAD and rAAVTeTxLC on the spastic mouse model of spasticity using behavioral and anatomical assays.

Rationale: The spastic mouse demonstrates the development of spastic tone and muscle/tendon contractures as the result of a mutation in the glycine receptor, which reduces the general inhibitory tone in the animal's nervous system. The application of BoNT-A to these animals has been documented to reduce contractures that develop in these animals secondary to spasticity throughout development. This model provides an approximation of human cerebral palsy. Two candidate vectors rAAVGAD and rAAVTeTxLC alter spinal cord tone by amplifying the production of GABA and reducing neuromuscular transmission respectively.
Experimental Design: Spastic phenotype mice will be selected from litters and paired with two non spastic litter mates on day 20 of life. Animals will be injected in the left sciatic nerve with 2 λ of the maximal titer of rAAVGAD, rAAVTeTxLC, or rAAVTeTxLCnt (n=20 per group). rAAVcagGAD (gift of During and Leone) contains the glutamate decarboxylase gene under the control of the CAG promoter. Animals will be evaluated for spasticity using a modified Ashworth Scale in the right and left leg by a blinded scorer as well as incline plane measurements on a weekly basis. Animals will be sacrificed on day 65 of life to undergo gastrocnemius to tibial ratio measurement.
Spastic Mice: B6C3Fe-a/a-Glrbspa/+ breeding pairs are purchased and bred. Litters are examined beginning at 14 days for homozygous spastic phenotype animals. The spasms consist of rapid tremor, stiffness of posture, and difficulty in righting when placed on the back. Litter mates can be selected as experimental controls.
Anesthesia: Mice are placed headfirst into a 30 cc syringe fitted into a 60 cc syringe attached to the open circuit gas anesthesia system. Isofluorane is administered as described in Aim #1.
Viral Injection: Virus will be injected in phosphate buffered saline (PBS) with 20% sucrose used as a cryoprotectant. Nerves are injected with an oocyte microinjector (Drummond: nanoject, Broomall, PA). A glass micropipette puller (Narishige: PP-83, Tokyo, Japan) is used to create tapered tips on micropipettes which are then beveled to a 100 μ diameter tip under microscopic visualization. Glass micropipettes are placed on the oocyte injector which is advanced through the perineurium along the axis of the nerve with the use of a micromanipulator (Narishige: N-152, Tokyo, Japan), while gentle counter traction is applied to the nerve. 0.5 λ is delivered in a series of ten 50 nl boluses, injected at four separate puncture sites for a total of 2 λ.
Blinded Examination for Spasticity: Using the modified Ashworth scale described by Bohannon and Smith (110), an individual blinded to the treatment category will score the degree of spasticity at the hip, knee, and ankle on a 0-5 scale as follows for the right and left limb score:

0=No increase in tone during flexion and extension
1=Catch and release or minimal resistance
2=Catch with minimal resistance
3=Increased tone throughout motion, easy movement
4=Considerably increased tone, difficult movement
5= Rigidity on flexion or extension

Gastrocnemius to Tibial Length Ratio: The degree of gastrocnemius contractures can be estimated in the spastic mouse model by measuring the length of the gastrocnemius and tibia and tabulating the ratios of these values for both hindlimbs.
Anticipated Results and Potential Problems: We anticipate that both rAAVGAD and rAAVTeTxLC sciatic therapy will result in reduced spasticity and contractures. We expect that rAAVTeTxLC will provide more robust effects than rAAVGAD. Further, it is likely that the injected limb will show disproportionate improvement in spasticity in comparison with the right limb. It is possible that rAAVTeTxLC may leave these animals with less spasticity and improvement in contractures but with more weakness. This should be apparent on incline plane assessment.

b. Evaluate the effect of sciatic nerve injections of rAAVGAD and rAAVTeTxLC on spinal cord contusion induced spasticity in Sprague-Dawley rats using behavioral and electrophysiological assays.

Rationale: Human spinal cord injury is rarely the result of focused lesions or transection. More commonly spinal cord injury results from cord crush or contusion. This trauma is one of the leading causes of spasticity. A range of spinal cord contusion severities can be induced with a weight drop model. The study of a larger rodent model allows for more sensitive assays of spasticity to be applied including electrophysiology and the measurement of dynamic limb resistance. Such assays will allow for better resolution of the dose response characteristics of antispasticity vector administration. The development of such therapies will depend on defining titers of virus that can reduce spasticity without exacerbating weakness.
Experimental Design: The therapeutic vector that performs better in the spastic mouse model will be selected for a more in depth characterization of dose-response characteristics. Groups of rats will undergo simultaneous left sciatic nerve vector administration and thoracic spinal cord injury. Animals in each treatment group, rAAVGAD or rAAVTeTxLC, and rAAVTeTxLCnt (n=15/group) will undergo a 5 cm weight drop injury and injection of 3 separate titers of virus 10^4, 10^6, 10^8 pt./µl. Dynamic force amplitude (DFA) and incline plane (as described in Aim 2a) assays will be measured biweekly for four weeks following injury. At the end of four weeks, animals will undergo measurement of bilateral monosynaptic reflex potentials (MSR) from the sciatic nerves. The ratio of MSR and dynamic force amplitudes in treated to untreated limbs will be calculated. These ratios will be compared between groups as well as the raw values of MSR and DFA.
Spinal Cord Injury: Based on the NYU weight-drop device (93) a spinal cord impounder was designed to deliver reproducible contusions to the spinal cord. The midthoracic spinal cord is exposed as described above. During the operation, the spinal cord impounder is positioned over the cord at the laminectomy defect. The spine is immobilized with modified Alice clamps fixed to the spinous processes rostral and caudal to the laminectomy. A 10 gram weight is dropped a standard distance along a track and strikes a teflon impounder tip that contuses the cord. The force transduced into the spinal cord can be measured with a tension transducer to insure consistent injury. Closure is performed as described above. Spinal cord injury results in partial or complete paralysis.
Dynamic Force Amplitude: A modification of the dynamic force amplitude apparatus described by Taylor et al (92) will be constructed in the machine shop of the Cleveland Clinic Lerner Research Institute. In brief, this apparatus utilizes an electric motor that rotates a wheel. This wheel is attached via a rod to a second wheel. This construction results in oscillation of the wheel similar to the principle that converts piston movement to rotary motion in locomotive wheels. The second wheel is connected to a fulcrum that is in turn attached to "boots." The final result is rhythmic dorsiflexion of the rat's feet at the ankle. Tension transducers are placed under the footpads to detect the resistance to dorsiflexion. The mean resistance to flexion over a series of trials can be calculated. In addition, the rate of dorsiflexion can be altered to look at the resistance/rate ratio.
Monosynaptic Reflex: Sprague-Dawley rats are intubated and induced under isofluorane anesthesia and animals are paralyzed with gallamine. The sciatic nerve is exposed bilaterally, severed and placed into a suction electrode for measurement of a nerve action potential. Lumbosacral laminectomy is performed and bilateral stimulating electrodes are placed on L3 dorsal roots which are severed distal to the stimulating electrode to prevent antidromic sensory stimulation from corrupting the sciatic nerve recording. Dorsal roots are stimulated with 50 µs pulses at 1 Hz. Sciatic recordings are amplified and averaged on a Nicolet 1170 Signal Averager over 10 trials. Scores are generated for both hindlimbs.
Anticipated Results and Potential Problems: We anticipate that the antispasticity vector but not rAAVTeTxLCnt will reduce DFA. We expect these results to last throughout the duration of the experiment, given that rAAV gene expression should not diminish over a single month. Further, we predict that antispasticity effects will be observed in the treated limb more than the contralateral side, but we do expect to see a degree of improvement in the contralateral limb, since some gene expression has been seen in the contralateral motor neurons. One potential problem is the possibility that the planned dose response curve will either miss peaks in the curve given the wide distribution of concentrations or will not utilize low enough doses. If the animals show worsened performance on the incline plane test at all dose levels, additional groups will be run at lower doses in an attempt to define the a dose that optimizes antispasticity effects without undermining the overall spinal cord function.

c. Construct and assay the activity of targeted rAAV for the delivery of antispasticity genes.
Rationale: Aim 3c attempts to synthesize the data on motor neuron targeting, antispasticity transgenes, and activity in animal models in order to demonstrate an increased effect of an antispasticity transgene using vector targeting. As previously stated, targeted capsids may allow for more potent and specific effects.
Experimental Design: rAAV2dec-*antispasticity* or rAAV2sstn-*antispasticity* will be constructed using the mutant pIM29-45 packaging helper plasmid found to perform better in Aim 3b. These two targeted antispasticity vectors will be compared to untargeted rAAV2-*antispasticity* (rAAVTeTxLC constructed in Aim

1 or rAAVGAD obtained from During and Leone). Three groups (n=5) of Sprague-Dawley rats will undergo sciatic nerve vector injection followed by 5 cm weight drop spinal cord injury. Incline plane performance, DFA, and MSA will be measured over a two month period.

Anticipated Results and Potential Problems: We predict that conjugated vectors will have the most dramatic motorneuron specific transgene delivery, because these vectors will not only have a high binding affinity for motorneurons, but will also be unlikely to bind surrounding tissue because their wildtype coat proteins will be hidden by the large neurotropic proteins. Targeted cap antispasticity vectors should likewise have a high affinity for remote uptake, but may not lose the ability to bind non-neural elements. The main potential problem remains the ability of targeted antispasticity vectors to cause synaptic inhibition at levels beyond the segmental area targeted. Once again, care will be taken to monitor the general spinal cord function of these animals including their respiratory function.

Broader Significance: The development of strategies for targeted gene delivery to motor neurons will be equally applicable to the attempt to develop gene therapy strategies for the treatment of Motor Neuron Disease. These therapies will be developed in collaboration with PFUND at the University of Michigan. In addition, local synaptic inhibition is currently being applied through the technology of deep brain stimulation to the treatment of movement disorders, epilepsy, eating disorders, and potentially psychiatric disease (see Appendix C) . Antispasticity vectors engineered to induce focused synaptic inhibition will provide biological strategies for stereotactic functional neurosurgery.

e. **Human Subjects**

None

f. **Vertebrate Animals**

1. Sprague-Dawley rats (Charles River) are anesthetized with sodium pentobarbital (65 mg/kg) and Spastic Mice (Jackson Labs, Maine) are anesthetized with inhalant isofluorane. For sciatic nerve injections, the lateral portion of the right thigh is shaved and sterilized with povidone-iodine. A 0.3 cm incision is made posterior to the right femur and the sciatic nerve is exposed and freed from surrounding tissue. All dissections are performed under a dissecting microscope (Stereozoom 6; Leica, Buffalo, NY). For some protocols, the brachial plexus or the laryngeal nerve are exposed after a 0.3 cm incision posterior to the neck or at the neck, respectively. Sciatic, brachial plexus and laryngeal nerve injections require a small amount of countertraction, accomplished by applying a loosely tied 3-0 silk suture around the nerve. The suture tails are cut and the remaining tie left in place following surgery for direct visualization of the injection site during tissue preparation. The amount of countertraction and retraction is carefully controlled to prevent nerve damage. 3-0 silk sutures are used to approximate the muscles and the skin is closed with a skin stapler (Reflex TL; Richard Allen, Richland, MI).

   To conduct direct spinal cord injections, using sterile technique, the paraspinous muscles of the L3 region are elevated from the lamina and spinous processes. A hemilaminectomy is performed using cuticle scissors at the midthoracic level. A micromanipulator is then used to insert a glass capillary tube beveled to 10 microns in diameter into the spinal cord at the midline. 4 lamda of viral solution is delivered using a nanoject oocyte injector apparatus. Par aspinous muscle is closed using a 3-0 vicryl suture and the skin is stapled. All staples will be removed 7-10 days after the procedure.

   To induce traumatic spasticity, spinal cord injury is induced with weight drop contusion model. Based on the NYU weight-drop device (93) a spinal cord impounder was designed to deliver reproducible contusions to the spinal cord. The midthoracic spinal cord is exposed as described above. During the operation, the spinal cord impounder is positioned over the cord at the laminectomy defect. The spine is immobilized with modified Alice clamps fixed to the spinous processes rostral and caudal to the laminectomy. A 10 gram weight is dropped a standard distance along a track and strikes a teflon impounder tip that contuses the cord. The force transduced into the spinal cord can be measured with a tension transducer to insure consistent injury. Closure is performed as described above. Spinal cord injury results in partial or complete paralysis. Such animals receive bladder massage three times a day until reflexive bladder control returns.

Animals are carefully monitored postoperatively for mutilation, urinary retention, and wound infection.

2. The mice will be housed in the Unit for Laboratory Animal Medicine (ULAM) of the Cleveland Clinic Foundation which is AALAC approved. ULAM provides a well-trained staff that is overseen by a Cleveland Clinic Foundation Veterinarian.

3. The use of sodium pentobarbital (65 mg/kg) or inhalant isofluorane anesthetizes the rodents during the surgery. The use of these anesthetics is consistent with the guidelines of the Panel on Euthanasia of the American Veterinary Medical Association and with NINDS guidelines.

g. **Literature Cited**

1. Krack P, Poepping M, Weinert D, Schrader B, Deuschl G. Thalamic, pallidal, or subthalamic surgery for Parkinson's disease? J Neurol 2000;247 Suppl 2:II122-II134
2. Wilson SP, Yeomans DC, Bender MA, Lu Y, Goins WF, Glorioso JC. Antihyperalgesic effects of infection with a preproenkephalin-encoding herpes virus. Proc Natl Acad Sci U S A 1999;96:3211-3216
3. Finkelstein R, Baughman RW, Steele FR. Harvesting the Neural Gene Therapy Fruit. Mol Ther 2001;3:3-7
4. Choi-Lundberg DL, Lin Q, Chang YN, Chiang YL, Hay CM, Mohajeri H, Davidson BL, Bohn MC. Dopaminergic neurons protected from degeneration by GDNF gene therapy. Science 1997;275:838-841
5. Castel-Barthe MN, Jazat-Poindessous F, Barneoud P, Vigne E, Revah F, Mallet J, Lamour Y. Direct intracerebral nerve growth factor gene transfer using a recombinant adenovirus: effect on basal forebrain cholinergic neurons during aging. Neurobiol Dis 1996;3:76-86
6. Boulis NM, Bhatia V, Brindle TI, Holman HT, Krauss DJ, Blaivas M, Hoff JT. Adenoviral nerve growth factor and β-galactosidase transfer to spinal cord: A behavioral and histological analysis. J Neurosurg (Spine 1) 1998;90:99-108
7. Boulis NM, Turner DE, Dice JA, Bhatia V, Feldman EL. Characterization of adenoviral gene expression in spinal cord after remote vector delivery. Neurosurgery 1999;45:131-138
8. Boulis NM, Noordmans AJ, Feldman EL, Imperiale MJ. Adeno-associated viral gene expression in the adult rat spinal cord following remote vector delivery. Mol Ther 2000;1(5):S110-S111
9. Wu P, Xiao W, Conlon T, Hughes J, Agbandje-McKenna M, Ferkol T, Flotte T, Muzyczka N. Mutational analysis of the adeno-associated virus type 2 (AAV2) capsid gene and construction of AAV2 vectors with altered tropism. J Virol 2000;74:8635-8647
10. Kozarsky KF, Wilson JM. Gene therapy: Adenovirus vectors. Curr Opin Genet Dev 1993;3:499-503
11. Neve RL. Adenovirus vectors enter the brain. Trends Neurosci 1993;16:252-253
12. Lawrence MS, McLaughlin JR, Sun GH, Ho DY, McIntosh L, Kunis DM, Sapolsky RM, Steinberg GK. Herpes simplex viral vectors expressing Bcl-2 are neuroprotective when delivered after a stroke. J Cereb Blood Flow Metab 1997;17:740-744
13. Breakefield XO, DeLuca NA. Herpes simplex virus for gene delivery to neurons. New Biol 1991;3:203-218
14. Peel AL, Klein RL. Adeno-associated virus vectors: activity and applications in the CNS. J Neurosci Methods 2000;98:95-104
15. Blomer U, Naldini L, Kafri T, Trono D, Verma IM, Gage FH. Highly efficient and sustained gene transfer in adult neurons with a lentivirus vector. J Virol 1997;71:6641-6649
16. Davidson BL, Doran SE, Shewach DS, Latta JM, Hartman JW, Rowssler BJ. Expression of Ecoli β-galactosidase and rat HPRT in the CNS of Macaca mulatta following adenoviral mediated gene transfer. Exp Neurol 1994;125:258-267
17. Baumgartner BJ, Shine HD. Targeted transduction of CNS neurons with adenoviral vectors carrying neurotrophic factor genes confers neuroprotection that exceeds the transduced population. J Neurosci 1997;17:6504-6511
18. Gimenez Y, Ribotta M, Revah F, Pradier L, Loquet I, Mallet J, Privat A. Prevention of motorneuron death by adenovirus-mediated neurotrophic factors. J Neurosci Res 1997;48:281-285
19. Liu Y, Himes BT, Moul J, Huang W, Chow SY, Tessler A, Fischer I. Application of recombinant adenovirus for in vivo gene delivery to spinal cord. Brain Res 1997;768:19-29
20. Boulis NM, Bhatia V, Anlar B, Brindle TI, Feldman EL. Retrograde adenoviral gene delivery to rat spinal cord via sciatic nerve microinjection. Society for Neuroscience Abstracts 1998;24(2):1308

21. Ghadge GD, Roos RP, Kang UJ, Wollmann R, Fishman PS, Kalynych AM, Barr E, Leiden JM. CNS gene delivery by retrograde transport of recombinant replication-defective adenoviruses. Gene Ther 1995;2:132-137
22. Durham HD, Lochmuller H, Jani A, Acsadi G, Massie B, Karpati G. Toxicity of replication-defective adenoviral recombinants in dissociated cultures of nervous tissue. Exp Neurol 1996;140:14-20
23. Yang Y, Su Q, Wilson JM. Role of viral antigens in destructive cellular immune responses to adenovirus vector-transduced cells in mouse lungs. J Virol 1996;70:7209-7212
24. Wood MJ, Charlton HM, Wood KJ, Kajiwara K, Byrnes AP. Immune responses to adenovirus vectors in the nervous system. Trends Neurosci 1996;19:497-501
25. Yang Y, Xiang Z, Ertl HC, Wilson JM. Upregulation of class I major histocompatibility complex antigens by interferon gamma is necessary for T-cell-mediated elimination of recombinant adenovirus-infected hepatocytes in vivo. Proc Natl Acad Sci U S A 1995;92:7257-7261
26. Byrnes AP, Wood MJ, Charlton HM. Role of T cells in inflammation caused by adenovirus vectors in the brain. Gene Ther 1996;3:644-651
27. Boulis NM, Turner DE, Imperiale MJ, Feldman EL. Neuronal survival following remote adenovirus gene delivery. J Neurosurg 2001; in press
28. Berns KI, Hauswirth WW. Adeno-associated viruses. Adv Virus Res 1979;25:407-449
29. Srivastava A, Lusby EW, Berns KI. Nucleotide sequence and organization of the adeno-associated virus 2 genome. J Virol 1983;45:555-564
30. Walsh CE, Liu JM, Xiao X, Young NS, Nienhuis AW, Samulski RJ. Regulated high level expression of a human gamma-globin gene introduced into erythroid cells by an adeno-associated virus vector. Proc Natl Acad Sci U S A 1992;89:7257-7261
31. Russell DW, Miller AD, Alexander IE. Adeno-associated virus vectors preferentially transduce cells in S phase. Proc Natl Acad Sci U S A 1994;91:8915-8919
32. Flotte TR, Afione SA, Zeitlin PL. Adeno-associated virus vector gene expression occurs in nondividing cells in the absence of vector DNA integration. Am J Respir Cell Mol Biol 1994;11:517-521
33. Berns KI, Linden RM. The cryptic life style of adeno-associated virus. Bioessays 1995;17:237-245
34. Samulski RJ, Chang LS, Shenk T. Helper-free stocks of recombinant adeno-associated viruses: normal integration does not require viral gene expression. J Virol 1989;63:3822-3828
35. Bueler H. Adeno-associated viral vectors for gene transfer and gene therapy. Biol Chem 1999;380:613-622
36. Kaplitt MG, Leone P, Samulski RJ, Xiao X, Pfaff DW, O'Malley KL, During MJ. Long-term gene expression and phenotypic correction using adeno-associated virus vectors in the mammalian brain. Nat Genet 1994;8:148-154
37. Peel AL, Zolotukhin S, Schrimsher GW, Muzyczka N, Reier PJ. Efficient transduction of green fluorescent protein in spinal cord neurons using adeno-associated virus vectors containing cell type-specific promoters. Gene Ther 1997;4:16-24
38. Klein RL, Meyer EM, Peel AL, Zolotukhin S, Meyers C, Muzyczka N, King MA. Neuron-specific transduction in the rat septohippocampal or nigrostriatal pathway by recombinant adeno-associated virus vectors. Exp Neurol 1998;150:183-194
39. Mandel RJ, Rendahl KG, Spratt SK, Snyder RO, Cohen LK, Leff SE. Characterization of intrastriatal recombinant adeno-associated virus-mediated gene transfer of human tyrosine hydroxylase and human GTP-cyclohydrolase I in a rat model of Parkinson's disease. J Neurosci 1998;18:4271-4284
40. Davidson BL, Stein CS, Heth JA, Martins I, Kotin RM, Derksen TA, Zabner J, Ghodsi A, Chiorini JA. Recombinant adeno-associated virus type 2, 4, and 5 vectors: transduction of variant cell types and regions in the mammalian central nervous system. Proc Natl Acad Sci U S A 2000;97:3428-3432
41. Chamberlin NL, Du B, de Lacalle S, Saper CB. Recombinant adeno-associated virus vector: use for transgene expression and anterograde tract tracing in the CNS. Brain Res 1998;793:169-175
42. Mandel RJ, Rendahl KG, Snyder RO, Leff SE. Progress in direct striatal delivery of L-dopa via gene therapy for treatment of Parkinson's disease using recombinant adeno-associated viral vectors. Exp Neurol 1999;159:47-64
43. Ruitenberg MJ, Dijkhuizen PA, Hermens WTJMC, Blits B, Schoenmakers N, van Heerikhuize JJ, et al. Adeno-associated viral vector-mediated gene transfer of brain-derived neurotrophic factor reverses atrophy of lesioned rubrospinal neurons. Society for Neuroscience Abstracts 1999;25:497
44. Xiao X, McCown TJ, Li J, Breese GR, Morrow AL, Samulski RJ. Adeno-associated virus (AAV) vector antisense gene transfer in vivo decreases GABA(A) alpha1 containing receptors and increases inferior collicular seizure sensitivity. Brain Res 1997;756:76-83

45. Rossmann MG. The canyon hypothesis. Hiding the host cell receptor attachment site on a viral surface from immune surveillance. J Biol Chem 1989;264:14587-14590
46. Muzyczka N. Use of adeno-associated virus as a general transduction vector for mammalian cells. Curr Top Microbiol Immunol 1992;158:97-129
47. Bartlett JS, Kleinschmidt J, Boucher RC, Samulski RJ. Targeted adeno-associated virus vector transduction of nonpermissive cells mediated by a bispecific F(ab'gamma)2 antibody. Nat Biotechnol 1999;17:181-186
48. Girod A, Ried M, Wobus C, Lahm H, Leike K, Kleinschmidt J, Deleage G, Hallek M. Genetic capsid modifications allow efficient re-targeting of adeno-associated virus type 2. Nat Med 1999;5:1052-1057
49. Rogers BE, Douglas JT, Ahlem C, Buchsbaum DJ, Frincke J, Curiel DT. Use of a novel cross-linking method to modify adenovirus tropism. Gene Ther 1997;4:1387-1392
50. Dmitriev I, Kashentseva E, Rogers BE, Krasnykh V, Curiel DT. Ectodomain of coxsackievirus and adenovirus receptor genetically fused to epidermal growth factor mediates adenovirus targeting to epidermal growth factor receptor-positive cells. J Virol 2000;74:6875-6884
51. Rancourt C, Rogers BE, Sosnowski BA, Wang M, Piche A, Pierce GF, Alvarez RD, Siegal GP, Douglas JT, Curiel DT. Basic fibroblast growth factor enhancement of adenovirus-mediated delivery of the herpes simplex virus thymidine kinase gene results in augmented therapeutic benefit in a murine model of ovarian cancer. Clin Cancer Res 1998;4:2455-2461
52. Tsiang H. Evidence for an intraaxonal transport of fixed and street rabies virus. J Neuropathol Exp Neurol 1979;38:286-299
53. Tuffereau C, Benejean J, Blondel D, Kieffer B, Flamand A. Low-affinity nerve-growth factor receptor (P75NTR) can serve as a receptor for rabies virus. EMBO J 1998;17:7250-7259
54. Seif I, Coulon P, Rollin PE, Flamand A. Rabies virulence: effect on pathogenicity and sequence characterization of rabies virus mutations affecting antigenic site III of the glycoprotein. J Virol 1985;53:926-934
55. Prehaud C, Coulon P, LaFay F, Thiers C, Flamand A. Antigenic site II of the rabies virus glycoprotein: structure and role in viral virulence. J Virol 1988;62:1-7
56. Coulon P, Ternaux JP, Flamand A, Tuffereau C. An avirulent mutant of rabies virus is unable to infect motoneurons in vivo and in vitro. J Virol 1998;72:273-278
57. Lentz TL, Wilson PT, Hawrot E, Speicher DW. Amino acid sequence similarity between rabies virus glycoprotein and snake venom curaremimetic neurotoxins. Science 1984;226:847-848
58. Kamata Y, Kimura Y, Hiroi T, Sakaguchi G, Kozaki S. Purification and characterization of the ganglioside-binding fragment of Clostridium botulinum type E neurotoxin. Biochim Biophys Acta 1993;1156:213-218
59. Binz T, Kurazono H, Popoff MR, Eklund MW, Sakaguchi G, Kozaki S, Krieglstein K, Henschen A, Gill DM, Niemann H. Nucleotide sequence of the gene encoding Clostridium botulinum neurotoxin type D. Nucleic Acids Res 1990;18:5556
60. Lalli G, Herreros J, Osborne SL, Montecucco C, Rossetto O, Schiavo G. Functional characterisation of tetanus and botulinum neurotoxins binding domains. J Cell Sci 1999;112 (Pt 16):2715-2724
61. Le Gall F, Favreau P, Benoit E, Mattei C, Bouet F, Menou JL, Menez A, Letourneux Y, Molgo J. A new conotoxin isolated from Conus consors venom acting selectively on axons and motor nerve terminals through a Na+-dependent mechanism. Eur J Neurosci 1999;11:3134-3142
62. Kharrat R, Mabrouk K, Crest M, Darbon H, Oughideni R, Martin-Eauclaire MF, Jacquet G, el Ayeb M, Van Rietschoten J, Rochat H, Sabatier JM. Chemical synthesis and characterization of maurotoxin, a short scorpion toxin with four disulfide bridges that acts on K+ channels. Eur J Biochem 1996;242:491-498
63. Cooper JR, Bloom FE, Roth RH. The Biochemical Basis of Neuropharmacology. New York: Oxford University Press, 1986
64. Gharakhanlou R, Chadan S, Gardiner P. Increased activity in the form of endurance training increases calcitonin gene-related peptide content in lumbar motoneuron cell bodies and in sciatic nerve in the rat. Neuroscience 1999;89:1229-1239
65. Talbot PJ, Dionne G, Lacroix M. Vaccination against lethal coronavirus-induced encephalitis with a synthetic decapeptide homologous to a domain in the predicted peplomer stalk. J Virol 1988;62:3032-3036
66. Turner DE, Noordmans AJ, Feldman EL, Boulis NM. Remote adenoviral gene delivery to the spinal cord: Contralateral delivery and reinjection. Neurosurgery 2001;48:1-9

67. Lance JW. Symposium synopsis. Feldman RG, Young RR, Koella WP, eds. Spasticity: disordered motor control. Chicago: Year Book Medical Publishers, 1980:485-494
68. Smyth MD, Peacock WJ. The surgical treatment of spasticity. Muscle Nerve 2000;23:153-163
69. Sherrington CS. Decerebrate rigidity and reflex coordination of movements. J Physiol (Lond) 1898;22:319-337
70. Hulliger M. The mammalian muscle spindle and its central control. Rev Physiol Biochem Pharmacol 1984;101:1-110
71. Schmidt RF. Motor systems. Schmidt RF, Thews G, Biederman-Thorson MA, eds. Human Physiology. Berlin: Springer, 1983:81-110
72. Pearson K, Gordon J. Spinal reflexes. Kandel ER, Schwartz JH, Jessell TM, eds. Principles of Neural Science. New York: McGraw Hill, 2000:713-735
73. Corcos DM, Pfann KD, Penn RD. Control of movement in parkinson's disease and spasticity: role of inhibition and excitation. Crockard A, Hayward R, Hoff JT, eds. Neurosurgery: the scientific basis of clinical practice. London: Blackwell Science, 2000:1218-1238
74. Young RR. Spasticity: a review. Neurology 1994;44:S12-S20
75. Burke D. Critical examination of the case for or against fusimotor involvement in disorders of muscle tone. Desmedt J, eds. Advances in Neurology vol. 39. Motor Control Mechanisms in Health and Disease. New York: Raven Press, 1983:133-150
76. Gilman S, Marco LA, Ebel HC. Effects of medullary pyramidotomy in the monkey. II. Abnormalities of spindle afferent responses. Brain 1971;94:515-530
77. Brown P. Pathophysiology of spasticity. J Neurol Neurosurg Psychiatry 1994;57:773-777
78. Dietz V. Spastic movement disorder. Spinal Cord 2000;38:389-393
79. Latash ML, Penn RD. Changes in voluntary motor control induced by intrathecal baclofen in patients with spasticity of different etiology. Physiother Res Int 1996;1:229-246
80. Johnson EA. Clostridial toxins as therapeutic agents: benefits of nature's most toxic proteins. Annu Rev Microbiol 1999;53:551-575
81. Davidson BL, Allen ED, Kozarsky KF, Wilson JM, Roessler BJ. A model system for *in vivo* gene transfer into the central nervous system using an adenoviral vector. Nat Genet 1993;3:219-223
82. Lilley CE, Groutsi F, Han Z, Palmer JA, Anderson PN, Latchman DS, Coffin RS. Multiple immediate-early gene-deficient herpes simplex virus vectors allowing efficient gene delivery to neurons in culture and widespread gene delivery to the central nervous system in vivo. J Virol 2001;75:4343-4356
83. Mitrophanous K, Yoon S, Rohll J, Patil D, Wilkes F, Kim V, Kingsman S, Kingsman A, Mazarakis N. Stable gene transfer to the nervous system using a non-primate lentiviral vector. Gene Ther 1999;6:1808-1818
84. Glorioso JC, Bender MA, Goins WF, DeLuca N, Fink DJ. Herpes simplex virus as a gene-delivery vector for the central nervous system. Kaplitt MG, Loewy AD, eds. Viral Vectors: Gene Therapy and Neuroscience Applications. San Diego: Academic Press, 1995:1-23
85. Thomas CE, Schiedner G, Kochanek S, Castro MG, Lowenstein PR. Peripheral infection with adenovirus causes unexpected long-term brain inflammation in animals injected intracranially with first-generation, but not with high-capacity, adenovirus vectors: toward realistic long-term neurological gene therapy for chronic diseases. Proc Natl Acad Sci U S A 2000;97:7482-7487
86. Naldini L, Blomer U, Gage FH, Trono D, Verma IM. Efficient transfer, integration, and sustained long-term expression of the transgene in adult rat brains injected with a lentiviral vector. Proc Natl Acad Sci U S A 1996;93:11382-11388
87. Peel AL, Zolotukhin S, Schrimsher GW, Muzyczka N, Reier PJ. Efficient transduction of green fluorescent protein in spinal cord neurons using adeno-associated virus vectors containing cell type-specific promoters. Gene Ther 1997;4:16-24
88. Kafri T, van Praag H, Gage FH, Verma IM. Lentiviral vectors: regulated gene expression. Mol Ther 2000;1:516-521
89. Bennett DJ, De Serres SJ, Stein RB. Regulation of soleus muscle spindle sensitivity in decerebrate and spinal cats during postural and locomotor activities. J Physiol 1996;495 (Pt 3):835-850
90. Taylor J, Munson J, Vierck CJ. Effects of dorsolateral spinal lesions on stretch reflex threshold and stiffness in awake cats. Eur J Neurosci 1999;11:363-368
91. Carter RL, Ritz LA, Shank CP, Scott EW, Sypert GW. Correlative electrophysiological and behavioral evaluation following L5 lesions in the cat: a model of spasticity. Exp Neurol 1991;114:206-215
92. Taylor JS, Friedman RF, Munson JB, Vierck CJJ. Stretch hyperreflexia of triceps surae muscles in the conscious cat after dorsolateral spinal lesions. J Neurosci 1997;17:5004-5015

93. Gale K, Kerasidis H, Wrathall JR. Spinal cord contusion in the rat: Behavioral analysis of functional neurologic impairment. Exp Neurol 1985;88:123-134
94. Yamamoto N, Takano H, Kitagawa H, Kawaguchi Y, Tsuji H. Changes of evoked action potentials and histology of the spinal cord, and hind limb dysfunction in spinal cord ischemia of cats. J Spinal Disord 1994;7:285-295
95. Simpson RKJ, Gondo M, Robertson CS, Goodman JC. The influence of glycine and related compounds on spinal cord injury-induced spasticity. Neurochem Res 1995;20:1203-1210
96. Pikov V, Gillis RA, Jasmin L, Wrathall JR. Assessment of lower urinary tract functional deficit in rats with contusive spinal cord injury. J Neurotrauma 1998;15:375-386
97. Ritz LA, Friedman RM, Rhoton EL, Sparkes ML, Vierck CJJ. Lesions of cat sacrocaudal spinal cord: a minimally disruptive model of injury. J Neurotrauma 1992;9:219-230
98. Kingsmore SF, Giros B, Suh D, Bieniarz M, Caron MG, Seldin MF. Glycine receptor beta-subunit gene mutation in spastic mouse associated with LINE-1 element insertion. Nat Genet 1994;7:136-141
99. Mulhardt C, Fischer M, Gass P, Simon-Chazottes D, Guenet JL, Kuhse J, Betz H, Becker CM. The spastic mouse: aberrant splicing of glycine receptor beta subunit mRNA caused by intronic insertion of L1 element. Neuron 1994;13:1003-1015
100. Chai CK. Hereditary spasticity in mice. J Hered 1961;52:241-243
101. Meier H, Chai CK. Spastic, an hereditary neurological mutation in the mouse characterized by vertebral arthropathy and leptomeningeal cyst formation. Exp Med Surg 1970;28:24-38
102. Chai CK, Roberts E, Sidman RL. Influence of aminooxyacetic acid, a gamma-aminobutyrate transaminase inhibitor, on hereditary spastic defect in the mouse. Exp Med Surg 1962;28:24-38
103. White WF, Heller AH. Glycine receptor alteration in the mutant mouse spastic. Nature 1982;298:655-657
104. Cohen RW, Fisher RS, Duong T, Handley VW, Campagnoni AT, Hull CD, Buchwald NA, Levine MS. Altered excitatory amino acid function and morphology of the cerebellum of the spastic Han-Wistar rat. Brain Res Mol Brain Res 1991;11:27-36
105. Baker D, O'Neill JK, Gschmeissner SE, Wilcox CE, Butter C, Turk JL. Induction of chronic relapsing experimental allergic encephalomyelitis in Biozzi mice. J Neuroimmunol 1990;28:261-270
106. Schluesener HJ, Sobel RA, Weiner HL. Demyelinating experimental allergic encephalomyelitis (EAE) in the rat: treatment with a monoclonal antibody against activated T cells. J Neuroimmunol 1988;18:341-351
107. Baker D, Pryce G, Croxford JL, Brown P, Pertwee RG, Huffman JW, Layward L. Cannabinoids control spasticity and tremor in a multiple sclerosis model. Nature 2000;404:84-87
108. Strong MJ, Garruto RM, Wolff AV, Chou SM, Fox SD, Yanagihara R. N-butyl benzenesulfonamide: a neurotoxic plasticizer inducing a spastic myelopathy in rabbits. Acta Neuropathol (Berl) 1991;81:235-241
109. Bertman LJ, Advokat C. Comparison of the antinociceptive and antispastic action of (-)-baclofen after systemic and intrathecal administration in intact, acute and chronic spinal rats. Brain Res 1995;684:8-18
110. Bohannon RW, Smith MB. Interrater reliability of a modified Ashworth scale of muscle spasticity. Phys Ther 1987;67:206-207
111. Lorenc-Koci E, Wolfarth S, Ossowska K. Haloperidol-increased muscle tone in rats as a model of parkinsonian rigidity. Exp Brain Res 1996;109:268-276
112. Ossowska K, Schulze G, Wolfarth S, Coper H, Kaminska A, Hausmanowa-Petrusewicz I. Muscle stiffness and continuous electromyographic activity in old rats; an animal model for spasticity? Neuroscience 1992;51:167-175
113. Cosgrove AP, Graham HK. Botulinum toxin A prevents the development of contractures in the hereditary spastic mouse. Dev Med Child Neurol 1994;36:379-385
114. Ziv I, Blackburn N, Rang M, Koreska J. Muscle growth in normal and spastic mice. Dev Med Child Neurol 1984;26:94-99
115. Grossman SP. Role of the hypothalamus in the regulation of food and water intake. Psychol Rev 1975;82:200-224
116. Fahn S. Regional distribution studies of GABA and other putative neurotransmitters and their enzymes. Roberts E, Chase TN, Towers DB, eds. GABA in Nervous System Function. New York: Raven Press, 1976:169-186
117. Tsujii S, Bray GA. GABA-related feeding control in genetically obese rats. Brain Res 1991;540:48-54

118. Mi J, Chatterjee S, Wong KK, Forbes C, Lawless G, Tobin AJ. Recombinant adeno-associated virus (AAV) drives constitutive production of glutamate decarboxylase in neural cell lines. J Neurosci Res 1999;57:137-148
119. Noordmans AJ, Song DK, Noordmans CJ, Boulis NM. Adeno-associated viral gene expression in the lateral nucleus of the rat hypothalamus. Society for Neuroscience Abstracts 2001;in press
120. Poulain B, Mochida S, Wadsworth JD, Weller U, Habermann E, Dolly JO, Tauc L. Inhibition of neurotransmitter release by botulinum neurotoxins and tetanus toxin at Aplysia synapses: role of the constituent chains. J Physiol (Paris) 1990;84:247-261
121. Tonello F, Pellizzari R, Pasqualato S, Grandi G, Peggion E, Montecucco C. Recombinant and truncated tetanus neurotoxin light chain: cloning, expression, purification, and proteolytic activity. Protein Expr Purif 1999;15:221-227
122. Davidson BL, Roessler BJ. Adenoviral-mediated gene transfer: potential therapeutic application. Kaplitt MG, Loewy AD, eds. Viral Vectors: Gene Therapy and Neuroscience Applications. San Diego: Academic Press, 2000:180-181
123. Rossetto O, Gorza L, Schiavo G, Schiavo N, Scheller RH, Montecucco C. VAMP/synaptobrevin isoforms 1 and 2 are widely and differentially expressed in nonneuronal tissues. J Cell Biol 1996;132:167-179
124. Kim B, Leventhal PS, Saltiel AR, Feldman EL. Insulin-like growth factor-I-mediated neurite outgrowth in vitro requires MAP kinase activation. J Biol Chem 1997;272:21268-21273
125. Soleilhac JM, Cornille F, Martin L, Lenoir C, Fournie-Zaluski MC, Roques BP. A sensitive and rapid fluorescence-based assay for determination of tetanus toxin peptidase activity. Anal Biochem 1996;241:120-127
126. Rivlin AS, Tator CH. Objective clinical assessment of motor function after experimental spinal cord injury in the rat. J Neurosurg 1977;47:577-581
127. Coco S, Raposo G, Martinez S, Fontaine JJ, Takamori S, Zahraoui A, Jahn R, Matteoli M, Louvard D, Galli T. Subcellular localization of tetanus neurotoxin-insensitive vesicle-associated membrane protein (VAMP)/VAMP7 in neuronal cells: evidence for a novel membrane compartment. J Neurosci 1999;19:9803-9812

h. **Consortium/Contractual Arrangements**

None

i. **Consultants**

Thyagarajan Subramanian MD holds a Staff level appointment in the Department of Neurology at the Cleveland Clinic Foundation. He holds an RO1 (NS42402) focused on the application of retinal stem cells and viral gene therapy to movement disorders. Dr. Subramanian will collaborate with Dr. Boulis in the development of gene therapy strategies for neuromodulation and neural restoration. In addition, Dr. Subramanian will assist Dr. Boulis in the development of strategies for the neural targeting of vectors. His basic science and clinical interests parallel those of Dr. Boulis making him an ideal collaborator.

Erwin Montgomery MD directs the Parkinson's Research Program at CCF. His basic science research utilizes primate models and electrophysiology to understand the complexity of the neural systems that regulate motor function. His clinical research focuses on early diagnosis and surgical treatment of Parkinson's disease. Dr. Montgomery will assist Dr. Boulis in the development of behavioral and electrophysiological assays of spasticity.

Michael Imperiale PhD is a Professor of Microbiology and Immunology and co-director of the Center for Gene Therapy at the University of Michigan. His laboratory investigates basic mechanisms of adenoviral pathogenesis including viral DNA packaging. He has assisted Dr. Boulis in the development of both adenoviral and rAAV vectors for IGF-I, GFP, and alkaline phosphatase (AP). Dr. Imperiale and the University of Michigan Center for Gene Therapy will continue to assist in the area of vector development and targeting.

Eva L Feldman MD. PhD is a Professor of Neurology at the University of Michigan. Her laboratory is focused on the application of neural growth factors to degenerative neurological diseases including diabetic neuropathy and motor neuron disease (ALS). She is the director of the Program For Understanding Neurologic Disease (PFUND). While a member of the faculty at the Cleveland Clinic, Dr. Boulis will maintain his position in the PFUND. Dr. Feldman will provide assistance with in vitro assays of vector activity including both SHSY5Y and primary motor neuron cultures.